RSC Advances

REVIEW

View Article Online
View Journal | View Issue

Cite this: *RSC Adv.*, 2024, **14**, 9406

Developments in conducting polymer-, metal oxide-, and carbon nanotube-based composite electrode materials for supercapacitors: a review

Aarti Tundwal,[a] Harish Kumar, *[a] Bibin J. Binoj,[a] Rahul Sharma,[a] Gaman Kumar,[a] Rajni Kumari,[a] Ankit Dhayal,[a] Abhiruchi Yadav,[a] Devender Singh [b] and Parvin Kumar[c]

Supercapacitors are the latest development in the field of energy storage devices (ESDs). A lot of research has been done in the last few decades to increase the performance of supercapacitors. The electrodes of supercapacitors are modified by composite materials based on conducting polymers, metal oxide nanoparticles, metal–organic frameworks, covalent organic frameworks, MXenes, chalcogenides, carbon nanotubes (CNTs), *etc.* In comparison to rechargeable batteries, supercapacitors have advantages such as quick charging and high power density. This review is focused on the progress in the development of electrode materials for supercapacitors using composite materials based on conducting polymers, graphene, metal oxide nanoparticles/nanofibres, and CNTs. Moreover, we investigated different types of ESDs as well as their electrochemical energy storage mechanisms and kinetic aspects. We have also discussed the classification of different types of SCs; advantages and drawbacks of SCs and other ESDs; and the use of nanofibres, carbon, CNTs, graphene, metal oxide–nanofibres, and conducting polymers as electrode materials for SCs. Furthermore, modifications in the development of different types of SCs such as pseudo-capacitors, hybrid capacitors, and electrical double-layer capacitors are discussed in detail; both electrolyte-based and electrolyte-free supercapacitors are taken into consideration. This review will help in designing and fabricating high-performance supercapacitors with high energy density and power output, which will act as an alternative to Li-ion batteries in the future.

Received 5th December 2023
Accepted 5th March 2024

DOI: 10.1039/d3ra08312h

rsc.li/rsc-advances

[a]*Dept of Chemistry, Central University of Haryana, Mahendergarh-123031, India. E-mail: harishkumar@cuh.ac.in*
[b]*Dept of Chemistry, MDU, Rohtak-124001, India*
[c]*Dept of Chemistry, Kurukshetra University, Kurukshetra, India*

1. Introduction

In recent decades, rapid globalization has increased the consumption of energy. At the global level, the human

Aarti Tundwal

Ms Aarti was born in Haryana, India, on July 25, 1997. She pursued a B.Sc. degree in Chemistry from the Maharishi Dayanand University Rohtak in 2017 and a Master's degree in Chemistry from the Central University of Haryana, Mahendergarh in 2019. She qualified CSIR-NET in 2020. She is currently working as a research scholar under the guidance of Prof. Harish Kumar at Central University of Haryana. Her research work is focused on conducting polymer-based nanocomposites and their applications.

Harish Kumar

Dr Harish Kumar is working as a Professor in the Dept. of Chemistry, School of Basic Sciences, Central University of Haryana, Mahendergarh (India). He has completed two major research projects. He has supervised 15 Ph.D. degrees. He is a member of different prestigious bodies. He has more than 19 years of teaching and research experience. He was awarded an international faculty exchange fellowship (Spain) and IISc, Bangalore, Summer Research Fellowship. He has granted 03 patents and published 03 patents. He has been awarded Indian Science Congress Science Communicator Award-2023. He has published 162 research papers, 04 books, and one monograph.

population is increasing at an alarming rate, raising energy requirements. The combined effect of these two factors leads to strain on the existing power infrastructure. Because of the rising usage of environmentally friendly and renewable energy systems in recent years, the consumption of hydrocarbon-based energy resources has decreased.[1] Automobiles, portable and non-portable electronic gadgets, fuel cells, *etc.* use electrochemical systems such as battery packs, supercapacitors (SCs), and bio-fuel cells to convert chemical energy into electrical energy or for energy storage.[2] A straightforward Ragone plot explains how batteries have moderated power and energy sectors, whereas SCs are thought of as elevated-power systems and fuel cells as high-energy systems (Fig. 1). The latest research is focused on the fabrication of SCs because of their unique properties, which has led to the testing of different composites as electrode materials such as carbon nanotubes (CNTs), conductive polymers (CPs), and metal oxide (MO) nanoparticles (NPs). The variety of uses of elastic and blendable SCs that need matching electrodes and components has led to the improvement of specific electrode materials.[3] It leads to environment-friendly and minimum-cost energy storage systems with emerging ecology and modern pollution free society.[4]

SCs are devices in which electrical energy can be stored *via* double-layer (DL) charging, faradaic reactions, or a combination of both. They are employed *via* thin dielectric layers and large surface area electrodes, which give high power density, outstanding periodic life, and a rapid charging/discharging rate, which in turn leads to high electrochemical performance.[5,6] The Leyden jar created in 1746, Netherlands, where electrical charges could be held on the plates of a so-called condenser, today known as a capacitor, was the first double-layer SC. The first patent, however, was only issued in 1957 and detailed a large surface area carbon-based capacitor.[7] SCs, their components, and their implementations are covered in a broader sense.[8–16] The rise in ED at the system level is mentioned in many articles published and has been emphasized about widely applicable outcomes.[17] The benefits of asymmetric and hybrid SC techniques have been explored along with the subsequent aspects.[18,19]

SCs play a major role in ESDs due to their unique characteristics and advantages. A few advantages of SCs over conventional batteries are as follows: (i) high power density: SCs can deliver and

Bibin J. Binoj

Bibin J. Binoj was born in Kerala, India, on July 8, 1999. He pursued his B.Sc. degree in Chemistry from Fatima Mata National College under Kerala University in 2021 and his Master's degree in Chemistry from the Central University of Haryana, Mahendergarh in 2023. He completed his dissertation work under the guidance of Prof. Harish Kumar at Central University of Haryana, Mahendergarh.

Rahul Sharma

Mr Rahul Sharma is pursuing his Ph.D. from the Central University of Haryana, Mahendergarh (India). He completed his Integrated M.Sc. Chemistry degree from NIT Rourkela (India) in the year 2016. He has qualified JRF NET (2018) and GATE (2022) examinations. He has published 17 research papers in reputed journals. He is currently working as a Guest faculty at the Central University of Haryana, Mahendergarh.

Gaman Kumar

Mr Gaman Kumar is from Mahendragarh, Haryana, India. He has completed his B.Sc. (Hon.) Chemistry from the University of Delhi in 2017 and M.Sc. Chemistry from Central University of Haryana in 2019. During his M.Sc., he qualified GATE exam in his first attempt in 2019. He achieved AIR-65 in GATE 2020. He also qualified CSIR UGC NET JRF 2019. He qualified GATE exam three times consecutively. Since, January 2022, he has been pursuing his Ph.D. from Central University of Haryana, India, under the supervision of Prof. Harish Kumar. He is currently working on the synthesis of flexible and conductive nanomaterial for multifunctional applications.

Rajni Kumari

Ms Rajni Kumari was born in 1996 in Charkhi Dadri, Haryana, India. She completed her B.Sc. from Kurukshetra University, India, (2015) and her M.Sc. in Physical Chemistry from Chaudhary Devi Lal University, India (2017). She has qualified CSIR-JRF (2018), CSIR-UGC-JRF (2019) and GATE (2019) examinations. Since, August 2019, she has been pursuing her Ph.D. from the Central University of Haryana, India, under the supervision of Prof. Harish Kumar. Her research work is focused on Nano-material-based electrochemical sensors and their applications.

absorb electrical energy at a much higher rate compared to batteries. Their high power density allows for quick charging and discharging, making them suitable for applications that require quick bursts of energy, (ii) long cycle life: SCs have an exceptionally long cycle life, with the ability to undergo hundreds to thousands or even millions of charge–discharge cycles,[9] (iii) efficient energy transfer: SCs show low internal resistance, and hence efficient energy transfer between the storage device and the load. This characteristic minimizes energy losses following charge and discharge cycles, leading to higher overall system efficiency,[10] (iv) wide temperature range: SCs can operate across a broad temperature range, from extreme cold to high heat, without significant degradation in performance.[12] This versatility makes them suitable for various environments and applications, including automotive, aerospace, and industrial sectors, (v) safety and environmental friendliness: SCs are generally considered safe due to their stable chemistry and lack of toxic materials. Unlike some battery chemistries, they do not pose significant risks of overheating, leakage, or explosion,[16] and (vi) complementary to rechargeable batteries: SCs can be used in conjunction with batteries to create hybrid energy storage systems that leverage the strengths of both technologies.[17,18] By combining the high EDs

Ankit Dhayal

Mr Ankit Dhayal was born in Rajasthan, India, on March 25, 1997. He pursued his B.Sc. degree in Chemistry Hons. from the University of Delhi in 2017 and a Master's degree in Chemistry from IIT Bombay in 2019. He is currently working as a research scholar under the guidance of Prof. Harish Kumar at Central University of Haryana. He qualified CSIR UGC-NET in 2017, 2018, and 2019 and GATE exam in 2019, 2020, and 2022. He is currently working in the field of biodegradable polymers and nanoparticles.

Abhiruchi Yadav

Ms Abhiruchi Yadav is from Rewari, Haryana, India. She completed her B.Sc. from Maharshi Dayanand University in 2016 and M.Sc. Chemistry from Central University of Haryana in 2019. She qualified GATE exam in 2020. Since, January 2022, she has been pursuing her Ph.D. from the Central University of Haryana, India, under the supervision of Prof. Harish Kumar. She is currently working on greener and sustainable approach to nanomaterial synthesis and their applications.

Devender Singh

Dr Devender Singh is working as Professor of Chemistry, Maharshi Dayanand University, Rohtak, Haryana (India). He has published 200 research papers in reputed national and international journals. He has completed SERB-DST and UGC funded major research projects. He has supervised eight scholars for their Ph.D. degrees. He has presented research papers on different national and international platforms. He is a member of different prestigious scientific academic bodies. He has more than 16 years of teaching and research experience. He was awarded international faculty exchange Marie Curie fellowship at Universidade do Minho, Braga, Portugal (2013 and 2014).

Parvin Kumar

Dr Parvin Kumar obtained his Master's degree in Organic Chemistry from the Department of Chemistry, Kurukshetra University, Kurukshetra, Haryana (India), in 2002. He received his Ph.D. in Chemistry from M. D. University, Rohtak, under the supervision of Prof. J. K. Makrandi in 2007. After completing his Ph.D., he joined as executive officer in the R&D lab of Bharat Rasayan Limited, Rohtak, and worked as senior executive officer. After that, he joined as an assistant professor in the GNKC, Yamuna Nagar (from July 2008 to Nov 2010). Since, Nov 2010, he has been working in the Department of Chemistry, Kurukshetra University, Kurukshetra, Haryana (India). Presently, he is working as Associate Professor. He has nearly 15 years of teaching and research experience. Four students have completed their Ph.D. under his guidance and four research scholars are currently working under his supervision. His area of research is synthetic organic chemistry, medicinal chemistry, enzyme inhibition, QSAR, docking, and other in silico *studies. He has published more than 150 research articles and 03 book chapters in national and international journals of repute.*

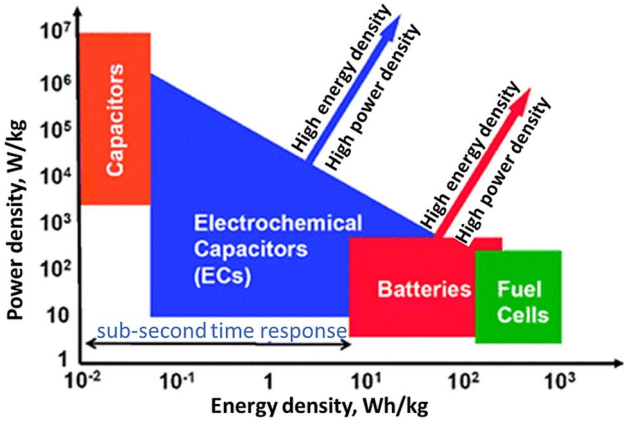

Fig. 1 Ragone graph of power density *vs.* energy density (ED) for different ESDs [Reproduced with permission from ref. 2. A copyright of RSC, 2008].

and power densities of batteries and the rapid response of SCs, these hybrid systems can enhance the overall performance, extending battery life and improving energy management.

Hence, SCs have high power density, long cycle life, efficient energy transfer, wide temperature range, safety, and environmental friendliness. These qualities make them indispensable in ESDs, supporting different applications where quick energy delivery, longevity, and reliability are essential requirements.

SCs may be divided into three types: Pseudo Capacitors (PCs), Electro-chemical Double Layer Capacitors (EDLC), and a hybrid kind produced by combining EDLCs and PCs (Fig. 2). Fig. 2 shows the working and internal structure of different types of SCs.

For the first time, we are introducing composite materials based on conducting polymers like polyaniline (PANI), polypyrrole (PPy), and polythiophene (PTh), CNTs [Single Walled Carbon Nanotubes (SWCNTs), and Multi-Walled Carbon Nanotubes (MWCNTs)] and transition MO NPs used in the fabrication of PCs, EDLCs, and SCs. Progress made towards development and modification done in increasing the charge storing capacity and ED of SCs by modifying the electrode material and electrolyte are discussed in detail. Kinetics and structural changes taking place at the surface of the electrode during the charging and discharging processes are discussed at full length. A comparison between rechargeable batteries and SCs is also made at relevant places. This review is mainly focused on the charge storage principle of SCs and the properties of modified electrode materials used in the latest SCs. This review is structured as SCs and their types, strategies of nanofiber (NF) fabrication, and different kinds of electrode materials used, including C material (graphitic carbon, graphene oxide, and CNTs), transition MO-based NF, and CP-based electrode materials used in SCs. The use of different MO/CPs-based composite as electrode materials (binary composite) in SCs is investigated in detail. NC materials are made of carbon along with MO NPs and CPs (tertiary composite) as the anode and cathode material. Lastly, we discussed the future scope and conclusions. This review article will certainly help researchers working in the field of ESDs to increase their performance and power output.

2. SCs as ESDs

SCs, also known as ultra-capacitors or electrochemical capacitors, are a type of ESD that stores electrical energy through the

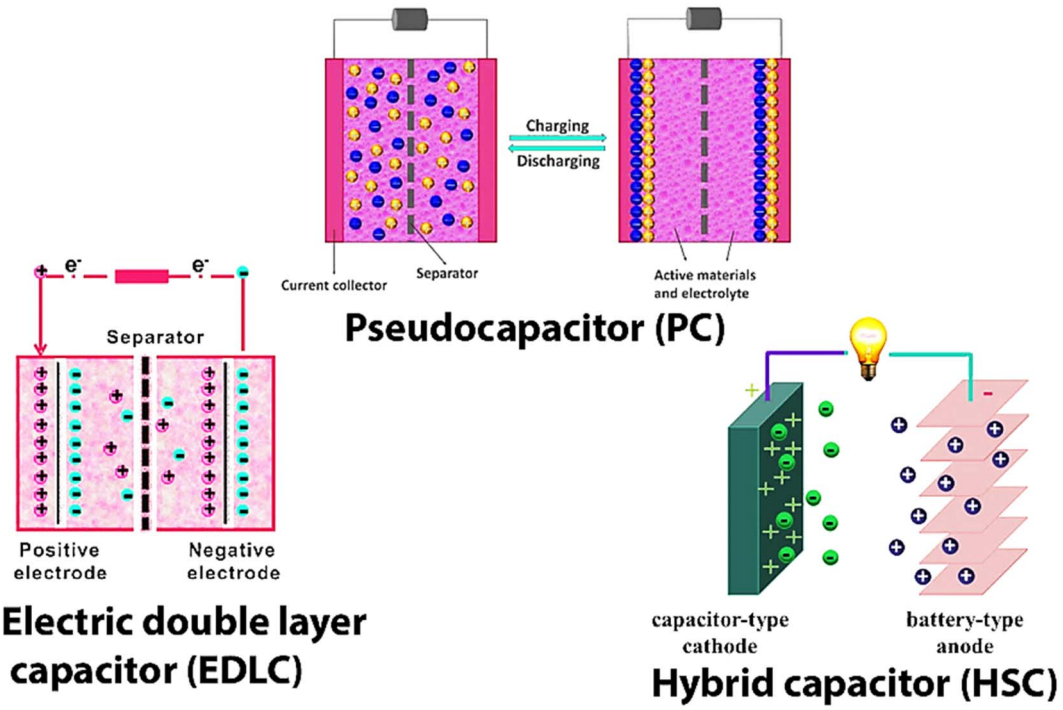

Fig. 2 Working and internal structure of different types of SCs.

electrostatic separation of charges at two plates. They are different from traditional rechargeable batteries and have different advantages over batteries like rapid charge and discharge capabilities and longer cycle life. SCs are classified based on their unique characteristics and applications as EDLCs, PCs, hybrid SCs, symmetric and asymmetric SCs, flexible and printable SCs, *etc.*

EDLCs store energy by forming an electric DL at the electrode–electrolyte interface. They have high power density, quick charge/discharge rates, and long cycle life. EDLCs are used for short-term energy storage, such as in regenerative braking systems, and peak power shaving in renewable energy systems. PCs store energy through fast and reversible faradaic reactions at the electrode–electrolyte interface. They offer higher EDs as compared to EDLCs but may have lower power density. Common electrode materials used in EDLCs are transition MOs (*e.g.*, RuO) and CPs.

Hybrid SCs combine the features of both EDLCs and PCs to provide a balance between energy and power density. These devices typically consist of an EDLC electrode and a PC electrode. Symmetric SCs have identical electrodes and are used for high-power applications.

Asymmetric SCs have different electrodes with varying properties to achieve a balance between energy and power density. Flexible and printable SCs are designed to be flexible, lightweight, and even printable on various substrates. They are used in wearable electronics, smart textiles, and other applications where traditional rigid SCs would be impractical. The choice of SC type depends on the specific requirements of the application, such as ED, power density, voltage range, and environmental conditions. Here, we will discuss a few important SCs used in ESDs.

2.1. EDLCs as ESDs

An electrolyte, a separator, and two electrodes made of C-based materials make EDLCs. EDLCs can conserve charge electrostatically when utilizing a non-faradaic technique that prohibits the charge from moving from the electrode to the electrolyte.[20–22] Electrochemical double layers are the basis for EDLCs' energy storage system. Ions in the medium migrate over the divider and the porous electrodes. When voltage is applied, as a consequence of the affinity between opposing charges generated by the potential difference. Ion recombination is prevented by an extra layer of charge which is built up at the electrodes. Electrodes composed of NCs possess a large Specific Surface Area (SSA), which provides a large surface for electrochemical reactions, ion recombination, charge storage capacity, *etc.* and hence, EDLCs show improved EDs.[23,24]

Additionally, the efficient storage mechanism of EDLCs enables much faster energy absorption, distribution, and increased production of power. Chemical reactions are prevented *via* the non-faradaic technique. It eliminates the swelling that occurs when rechargeable batteries, especially Li-ion batteries (LIBs), are charged and drained due to the active substance present as an electrolyte.

There are a few key distinctions between EDLCs and rechargeable batteries, that is, (i) batteries can only survive a few thousand cycles at best, but EDLCs can have large cycle life, and (ii) in EDLCs, the electrolytic solvent does not contribute significantly to the charge storage process; instead, it increases ionic mobility and minimizes resistance between the two electrodes. However, Solid-State Electrolytes (SSEs) have some contribution to increase the charge storage capacity of EDLCs.[25–30] EDLC devices only have small EDs due to the electrochemical surface charging mechanism. Because of this, the majority of recent research on EDLCs has focused on improving energy efficiency and extending the temperature range in which batteries cannot work. The effectiveness of EDLCs can be influenced by the type of electrolyte used.

2.2. Pseudocapacitors (PCs)

PCs are a type of ESD that combines the principles of traditional capacitors and rechargeable batteries. They are designed to provide high EDs and rapid charge/discharge capabilities, making them ideal for a large number of applications. In the 1960s, the pseudo-capacitance concept was introduced to understand surface faradaic processes like hydrogen evolution and underpotential deposition (UPD). UPD is defined as the electrodeposition of metal monolayers onto a different metal substrate at less negative potential than the electrodeposition of the same metal as the substrate.[21] The CV shows significant and highly reversible peaks due to the formation of different structures of the electrodeposited monolayers on the surface of the electrode.

Compared to electrostatically charged EDLCs, PCs use the faradaic principle to store charge, which includes the exchange of charges between the two electrodes.[24] The cycling stability of SCs was found to be intermediate between LIBs and EDLCs. If a voltage is supplied in a PC, the electrode material undergoes reduction and oxidation. A faradaic current flows *via* the SC electrodes as a result of the transfer of charge *via* the DL. Due to the involvement of the faradaic principle to store the charge, PCs can reach higher specific capacity and EDs than EDLCs. MO NPs and CPs are two examples that are used in PCs to increase charge-storage capacity.[25] This raises the interest of researchers in these materials, but they also possess cyclical instability and low power density due to their faradaic nature, which necessitates a reduction–oxidation process comparable to that of batteries.[31–33]

Fig. 3 shows different types of electrochemical energy harnessing methods which depend on capacity which influences the degree of electrode surface modification (structural changes), over-potential, and types of electrode kinetics. The main advantage of PCs is their short cycle life ranging from 10 seconds to 10 min.

The kinetic behavior of a battery involves chemical reactions that occur during the charge and discharge processes. These reactions typically involve the insertion and extraction of ions or molecules into/from the electrode materials. PCs exhibit faster kinetics than batteries because their charge and discharge processes involve rapid surface redox reactions, which do not require the diffusion of ions deep into the electrode material. Batteries have slower charge and discharge rates compared to PCs due to the relatively sluggish nature of the chemical reactions involved. This slower kinetics is a limiting factor in

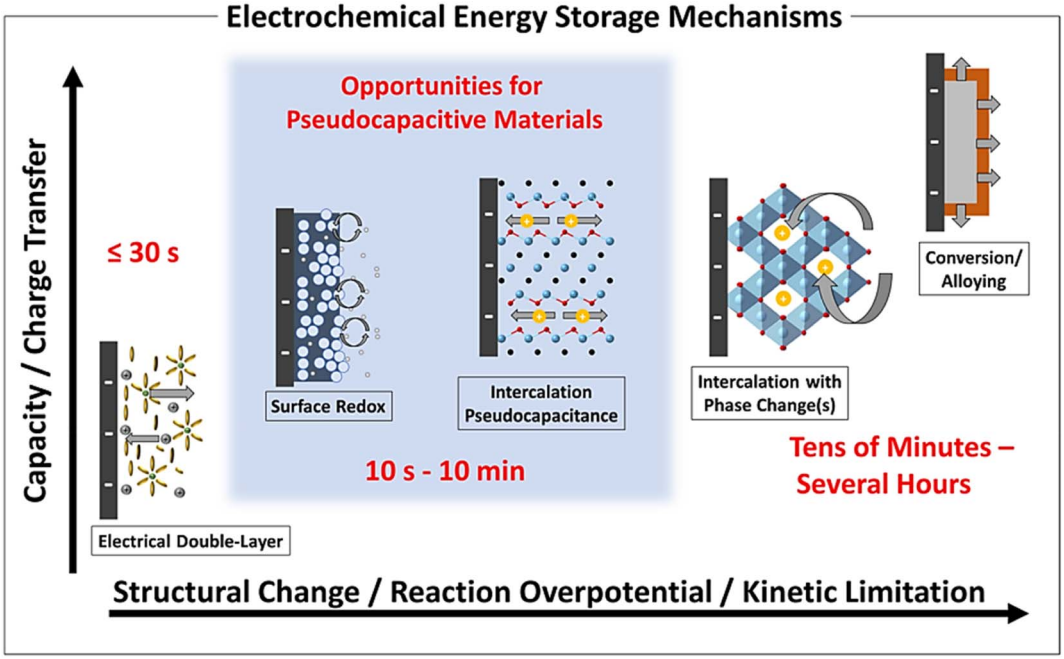

Fig. 3 Different electrochemical energy harnessing mechanisms of PCs as a function of characteristic capacity, degree of structural modifications in the electrodes, reaction over-potential, and limits of the chemical kinetics [Reproduced with permission from ref. 30. A copyright of ACS, 2020].

applications that require rapid energy exchange. However, PCs can deliver and store electrical energy quickly, making them suitable for applications requiring rapid energy cycling, such as regenerative braking in vehicles.

Batteries often undergo significant structural changes during charge and discharge cycles. For example, in LIBs, the anode and cathode materials can expand and contract as Li ions intercalate and de-intercalate, leading to mechanical stress and eventual electrode degradation.

The structural changes during the charging and discharging of batteries can limit their cycle life, as repeated expansion and contraction lead to electrode cracking and capacity fading with time. PCs typically undergo minimal structural changes during charge and discharge processes because their energy storage primarily relies on surface redox reactions. There is less volume change in the electrode materials compared to batteries. PCs often have longer cycle lives compared to batteries due to the reduced mechanical stress on the electrode materials. This makes them more durable and capable of withstanding a large number of charge–discharge cycles.

PCs are mainly composed of two components: electrodes and an electrolyte. The electrodes in PCs are made of highly conductive materials, such as Activated Carbon (AC), graphene, CNT, CP, and MO-based composites, which provide a large surface area for electrochemical reactions.[34–37] The quick charge transfer reactions due to the adsorbed species on the electrode surface depend upon UPD, intermediates adsorbed on ions present in the electrolyte, and electrode composition.[28] The electrolyte is a liquid or gel-like substance containing ions that facilitate the charge transfer between the electrodes. The working principle of PCs is based on two electrochemical processes that are double-layer capacitance (C_{dl}) and redox reactions. C_{dl} is produced in PCs when a voltage is applied across the electrodes which results in the formation of an electrical DL at the electrode–electrolyte (e–i) interface. The DL comprises two regions: the Helmholtz–Perrin and diffuse-charge layers. The Helmholtz–Perrin layer regularly contains tightly bound ions (in a plane), while the diffuse charge layer contains loosely bound randomly arranged ions. The separation of charges at the e–i interface creates a DL capacitance (C_{dl}), which allows for the rapid storage of charge and instantaneous release of electrical energy. In addition to DL capacitance, PCs also exhibit pseudo-capacitance resulting from reversible faradaic redox reactions.[37] This involves the transfer of electrons between the two electrodes. The electrode material undergoes oxidation and reduction reactions during the charging and discharging of PCs. This redox reaction chemistry contributes to the overall capacitance of the PC and hence increases its total energy storage capacity. Fig. 4 shows different types of pseudocapacitance mechanisms that is adsorption, electrochemical, and intercalation. The shape and area of the CV region demonstrate the differences in the electrochemical performance of SCs.

The combination of C_{dl} and pseudo-capacitance enables PCs to achieve higher energy storage densities than traditional capacitors while maintaining fast charge/discharge cycles. The working principle of PCs involves the process of charging and discharging. During charging, when a voltage is applied, ions from the electrolyte are attracted to the electrode surfaces, creating a DL. Simultaneous redox reactions take place, leading

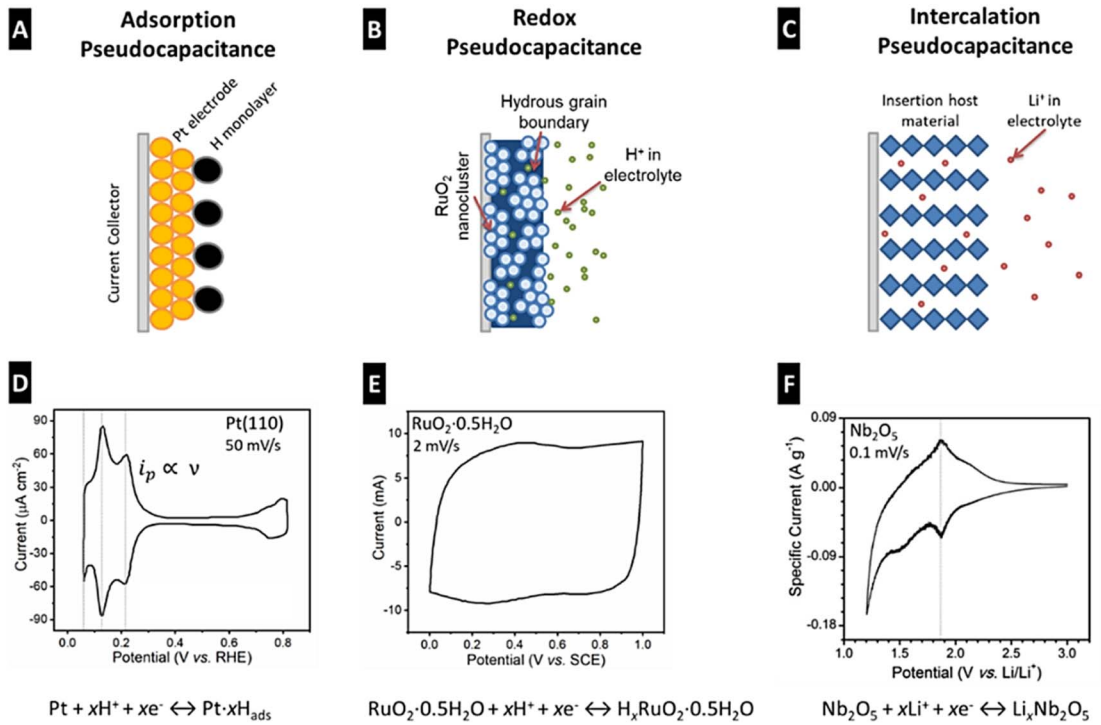

Fig. 4 Different types of pseudo-capacitance mechanisms: adsorption (A), electrochemical (B), and intercalation (C). CV of the Pt (110) electrode in $HClO_4$ solution at 50 mV s^{-1} *versus* SHE (D). CV of $RuO_2 \cdot H_2O$ in H_2SO_4 at 2 mV s^{-1} w.r.t. SCE (E). CV of the Nb_2O_5 electrode in non-aqueous Li-ion electrolyte at 0.1 mV s^{-1} w.r.t. SCE (F). The area in the CV cover was the maximum for electrochemical type SCs [Reproduced with permission from ref. 30. A copyright of ACS, 2020].

to the reversible storage of charges in the form of ions at the e–i interface. This results in the accumulation of electrical energy in the PCs. During discharging, the stored charges are released, and the ions return to the electrolyte, generating a flow of electrons through an external circuit. This discharge process can occur rapidly, enabling high-power delivery when needed.

PCs offer many advantages as compared to other ESDs, which include the following: (i) high power density: PCs can deliver and store energy rapidly due to the C_{dl} and redox reaction chemistry, (ii) long cycle life: PCs possess excellent cycle life with minimal degradation, making them suitable for long-lasting applications, (iii) high operating temperature range: PCs can operate in a wide range of temperatures, increasing their applicability in different environments, and (iv) high EDs: PCs have higher energy storage capacities than traditional capacitors, although they generally have lower EDs as compared to rechargeable batteries.

The first RuO_2 transition metal oxide-based PCs were reported by Transatti *et al.* in 1971.[13] The high cost of RuO_2 limits its large-scale production. Later, in 1999, amorphous $MnO_2 \cdot nH_2O$ in neutral aqueous solution-based PCs showed better performance.[26] The observed specific capacitance was 200 F g^{-1} in KCl solution. In the late 1980s, CP-based PCs were developed.[27] The theoretical capacity of PANI-based PCs was 146 mA h g^{-1}.[31] Carbon/CP based NC electrode materials were also used in PCs to increase the theoretical capacity of PCs.[38,39] In the 1980s, Li-ion intercalation was tested using organic electrolytes.[40] The discovery of carbon nitrides that is $Ti_3C_2T_x$ (MXenes), a new electrode material for PCs, led to an increase in the electrochemical performance of PCs.[15] This choice was driven by the remarkable properties exhibited by MXenes, including exceptional electrical conductivity,[41] electrochemical activity, hydrophilicity, environmentally benign nature, layered shape, large surface area, and thermal stability.[42,43]

PCs find applications in many fields, like energy storage systems, hybrid vehicles, renewable energy systems, portable electronics, and grid-level energy storage. They are particularly useful in situations where high power delivery and rapid charging/discharging are essential requirements.

2.3. Hybrid capacitors (HCs)

In PCs, EDLCs offer higher specific capacity while also having great periodic stability and power performance. In HCs, the hybrid system delivers a combination of both blending a power source that is an electrode that functions like a capacitor and a source of energy that is an electrode that functions like a battery in the same cell.[35,36] HCs, also known as asymmetric capacitors, are a type of ESD that combines the features of both capacitors and rechargeable batteries. They are designed to provide a balance between high power density (like capacitors) and high EDs like LIBs, making them suitable for applications that require both rapid charge/discharge capabilities and long-term energy storage.

By raising the cell voltage with the appropriate electrode composition, the ED and power density of HCs may be improved. In the past, many combinations of aqueous and inorganic electrolytes with positive and negative electrodes have

been investigated. The faradaic electrode frequently boosts the ED at the price of cycle stability. This is the main limitation of hybrid devices contrasted to EDLCs.[37]

HCs consist of two main components: an EDLC electrode and a battery electrode. The EDLC electrode is typically made of a high conductivity material with a large SSA, like AC, graphene, or CNTs. The battery electrode is composed of a high-capacity material, such as an MO or a CP. A separator separates both electrodes and is exposed to an electrolyte. The working principle of HCs is based on the combination of an electrochemical DL capacitance and battery-like faradaic reactions. Similar to traditional SCs, HCs utilize the principle of C_{dl}. When a voltage is applied, an electrical DL forms at the e–i interface between the EDLC electrode and the electrolyte. The charge separation at this interface creates a DL capacitance, allowing for rapid charge and discharge of electrical energy. In addition to C_{dl}, HCs also exhibit faradaic reactions at the battery electrode. The battery electrode undergoes reversible redox reactions during the charging and discharging processes. These reactions involve the transfer of charge between the two electrodes and the electrolyte, leading to the charge storage and release of electrical energy.[38] The faradaic reactions contribute to the overall energy storage capacity of the HCs. The combination of C_{dl} and faradaic reactions allows HCs to achieve a balance between high power density and high ED.[39–41] The operation principle of HCs involves charging and discharging reactions. During charging, a voltage is applied for a fixed duration, and opposite charges are attracted to the EDLC electrodes, leading to the formation of an electrified interface. Simultaneously, faradaic reactions occur at the battery electrode, enabling the reversible storage of charges at the electrode surface. This results in the accumulation of electrical energy in the HCs. During discharging, the stored charges are released. The discharge process involves reciprocal redox reactions at the battery electrode and the release of charges from the electrified interface at the EDLC electrode. This discharge process can occur rapidly, providing high-power delivery when needed.[42]

HCs have many advantages as compared to traditional capacitors and rechargeable batteries, which are as follows: (i) high power density: HCs can deliver and store energy rapidly due to the combination of C_{dl} and faradaic reactions, (ii) high EDs: HCs provide a higher energy storage capacity compared to traditional capacitors, although typically lower than rechargeable batteries, and (iii) long cycle life: HCs exhibit excellent cycle life, with minimal degradation over multiple charge/discharge cycles. HCs find applications in many fields, including electric vehicles, renewable energy systems, portable electronics, and power backup systems. They are particularly useful in applications that need great power and energy storage for longer duration, striking a balance between the capabilities of capacitors and batteries. The present research focuses on the three primary types of hybrid SCs—composite, asymmetric, and battery-type—which may be distinguished by their electrode topologies.

2.4. Composite hybrid SCs

To generate a single electrode that can collect charges both physically and chemically, electrodes are composed of AC and MO or CP-based materials. The highly porous structure of AC imparts a C_{dl} of high charge and SSA to enhance the interfacial interaction between pseudo-capacitive materials and the electrolyte. By using the faradaic process, pseudo-capacitive materials increase the capacitance of the composite electrode. Two-fold and three-fold composite materials are commonly used in HCs. Whereas ternary composites utilize three distinct electrode materials, a single electrode and binary composite electrode employ two independent electrode materials. Every composite falls into a variety of size categories, such as nanometers, micrometers, sub-micrometers, *etc.*[38]

Composite hybrid SCs combine the advantages of both traditional electrochemical SCs and rechargeable batteries, offering high ED and power density. Some key areas of progress in the development of composite hybrid SCs include the following: (i) material development: researchers are constantly exploring different advanced materials to improve the performance of SCs. For example, graphene and other carbon-based materials have been widely investigated due to their excellent electrical conductivity and large surface area, which will increase energy storage capacity, (ii) nanostructured electrode materials: the use of nanostructured electrode materials has shown promise in enhancing the energy storage capacity of SCs. By employing nanomaterials, such as CNTs or MO NPs, CPs, MXenes, *etc.*, researchers have increased the surface area available for charge storage, leading to improved capacitance,[39] (iii) hybridization with rechargeable batteries: combining SCs with rechargeable batteries in a hybrid configuration has gained attention as a means to achieve high EDs and power densities. This approach combines the high energy storage capacity of rechargeable batteries with the high power density and rapid charge/discharge capabilities of SCs, (iv) advanced electrolytes: electrolytes play a crucial role in the performance of hybrid SCs. Researchers have been exploring the use of novel electrolytes, such as ionic liquids or gel electrolytes, to improve the ED and stability of composite hybrid SCs, and (v) device architecture: optimizing the device architecture is another avenue of progress done in hybrid SCs. Researchers are developing innovative designs, such as asymmetric SCs or interdigitated structures, to enhance overall performance by maximizing energy and power densities. It's worth noting that the field of energy storage is actively evolving, and a lot of progress has been made in increasing the ED and the power density of composite hybrid SCs.

2.5. Asymmetric hybrid capacitors

Asymmetric HCs merge faradaic and non-faradaic reactions by coupling EDLCs with an electrode for PCs. The positive electrode is made up of CPs or MOs and the negative electrode is composed of C-based materials.[41]

2.6. Battery-type hybrid capacitors

Battery-type HCs, like asymmetric hybrids, combine two distinct electrodes. In this type of hybrid capacitor, the electrodes from the battery and the SCs are joined. The advantages of batteries and SCs were combined in one capacitor using the design shown in Fig. 2.

The energy storage and release mechanism of the EDLCs occurs at the electrified interface, which is created electrochemically. The lack of chemical oxidation–reduction (redox) processes renders the non-faradaic charge storage mechanism. EDLCs possess increased cycle lifetimes since only physical charge transfer occurs during the process. PCs, on the other hand, are built using high-energy electrode materials that are composed of CPs, metal-doped C, or metal oxides. In faradaic redox reactions, these CP and C-based materials are used.[39–42] These electrode materials enable the development of SCs with higher EDs. When compared to EDLCs, PCs frequently have higher EDs but also have shorter cycle lives and slower speeds. As mentioned, both EDLC and PC processes are present in the hybrid SCs.

The basic building block of an SC includes the two electrodes segregated from one another by a selectively permeable membrane acting as a separator (Fig. 2). The electrodes and separator are impregnated with an electrolyte solution, which permits ionic current to flow between them while obstructing electronic current from the cell. Current collectors receive current from the electrodes. The same equations that govern regular capacitors also apply to SCs, and the capacitance may be computed from the conventional capacitance, which would be calculated using eqn (1).

$$C = \frac{\varepsilon_0 \varepsilon_r A_e}{d} \quad (1)$$

where A_e is the geometrical electrode surface area, ε_0 is the space permittivity, ε_r is the relative permittivity of the material used in dielectrics, and d is the distance between two electrodes with opposing bias.

The SCs may be made from diverse materials depending on the type of energy storage required for the task and the necessary capacitance ranges. The major commercial material for SCs is carbon, which is widely used and has a wide range of potential transformations. There is currently a huge variety of materials suitable for SCs. MO like Ni, Co, Mn, and Ru are commonly used. In recent years, the usage of CNTs and CPs in SCs has increased (Fig. 5). SCs are significantly more advantageous than rechargeable batteries because of the novel materials used in the fabrication of electrode materials (Table 1).[43,44] Table 1 shows the advantages and disadvantages of SCs and other ESDs.

Nonetheless, SCs provide the required instant current and minimize the battery current in the event of transitory power interruption. The SCs may act as a complement to the present battery technology. To compensate for transitory and momentary disturbances, large battery units can be used parallel to electrochemical SCs. This would considerably lessen the unnecessary strain placed on batteries from frequent interruptions.[49] Recent SC research has exclusively focused on figuring out how to preserve high power density, quick charge/discharge, and cycle stability while increasing EDs.[50,51]

2.6.1. Nanofibers (NFs) used as electrode materials in SCs. NFs can be fabricated using a variety of techniques, including plasma-based synthesis, chemical vapor deposition (CVD), dry-spinning, gel spinning, wet-spinning, centrifugal jet spinning, solution blow spinning, and the hydrothermal approach.[52–63]

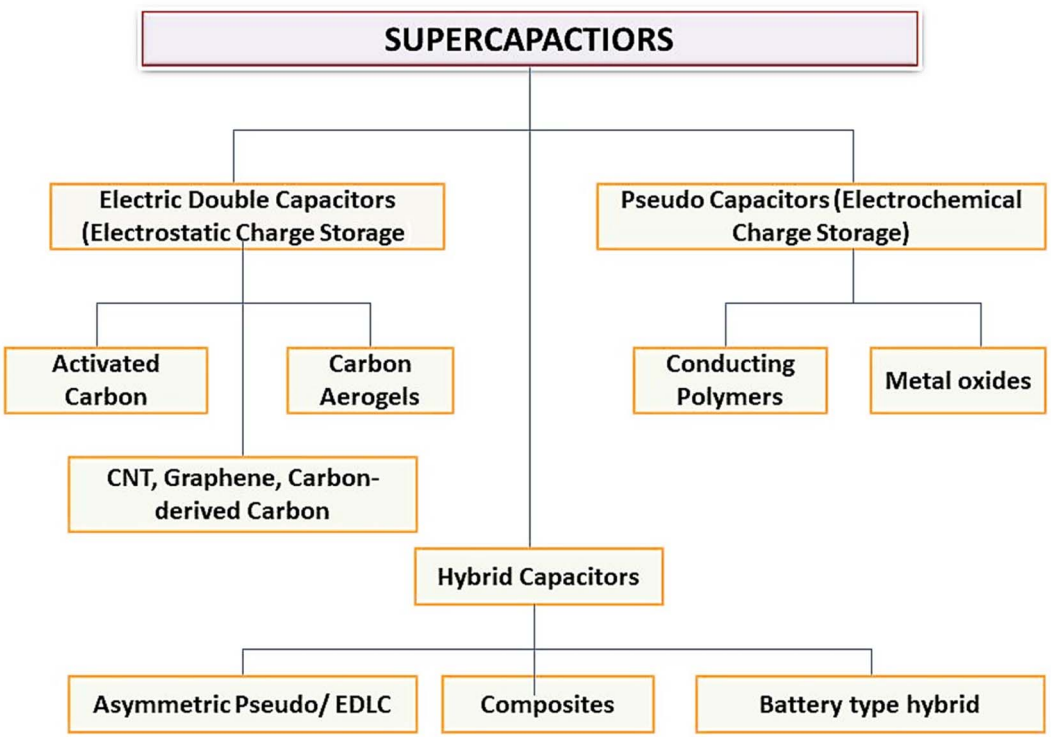

Fig. 5 Classifications of different types of SCs.

Table 1 Benefits and drawbacks of SCs and other ESDs

Types	Benefits	Drawbacks	References
SCs	(i) High power density (ii) Extended cycle life (iii) Quick charging speed (iv) Effective performance at low-temperature (v) Efficient charging and discharging circuit	(i) Lesser EDs (ii) Spontaneous discharge	39–42
LIBs	(i) Enlarged-working platform (ii) High EDs (iii) Extended periodic stability (iv) Efficient charging and discharging (v) Good safety at room temperature, zero carbon emission (vi) Can perform at a wide temperature range	(i) The cost of Li metal is high due to the relatively lower abundance (ii) Overcharging and over-discharging line management are required	45 and 46
Lithium sulfur batteries (LSBs)	(i) Higher EDs (ii) High theoretical capacity (iii) Less toxic and environmental preservation (iv) Good charge–discharge efficiency (v) Log cycle life	(i) Low-performance rate (ii) Poor Coulomb efficiency poorly stable cycles	47 and 48
Na-ion batteries (SIBs)	(i) EDs comparable to LIBs (ii) Better stability (iii) Better safety records (iv) Extended service life (v) Easy access to raw materials (vi) The ability of SIBs to discharge to 0 V due to lack of over-discharge characteristics	(i) Compared to LIBs, SIBs have a slow charge–discharge rate (ii) Large size and weight compared to LIBs (iii) Low EDs compared to LIBs (iv) SIBs require different anode material as compared to carbon in LIBs	172

The repeatability of the NFs as prepared can be hampered by the type of processes, which are comparatively time-consuming, expensive, and sophisticated.[52] A simple and rapid approach to producing NFs is required.[53] The electrospinning (ES) approach has become widely used due to its adaptability for commercial manufacture, simplicity, and ability to create configurable features (diameter, morphology, and composition).[54] The ES configuration, the method of producing NFs,[55] and the factors affecting the morphology of the fibrils are therefore briefly summarized in subsequent sections.

2.6.2. ES approach of synthesis of NFs. For the most part, a standard ES setup requires four components, as illustrated in Fig. 6, a spinneret with a small spine, a syringe, a potential source (kV), and a fiber collector. The vertical ES setup (the stationary mode-b) and the horizontal ES setup (the vibrant mode-a) are the two divisions of the ES configuration. The high-voltage source is attached to a syringe containing molten metal or a solution of a polymer with a pendant droplet. The ES solution is released as threads to the collector at a set flow rate that is controlled by a syringe pump. The polymeric droplet's hemispherical surface is charged due to electrostatic interactions and then stretched until it assumes the shape of a Taylor cone.[55] The surface tension of the polymeric solution is released at a threshold voltage, dissipating enough force produced by electrostatic interactions to cause a continuous jet to depart the spinneret and go to the collector. When the repellent power between the electrified jets grows stronger, it causes more bending instability and elongation, which leads to the development of thinner fibers. After that, the jet gradually evaporates and hardens, producing continuous ES fibers.

The primary factors that affect the morphology of the ES fibers are the tip-collector distance, applied voltage, flow velocity, and the polymeric solution's viscosity.[56] Additionally, the assembly of the fibers may be accomplished by utilizing a variety of collector types. For instance, static collectors are used to construct fibers with a web-like structural morphology, whereas cylindrical spinning drum collectors are used to create non-woven fibers.[57,58]

2.6.3. Carbon NFs used as electrode materials in SCs. The SCs depend on the EDLC and type of electrodes that is graphene oxide, carbon aerogels, activated charcoal, CNTs, and carbon nanofibres (CNFs), which possess exceptional properties due to consistent electrochemical activity over an extended period. With their potential to offer improved electrical conductivity,

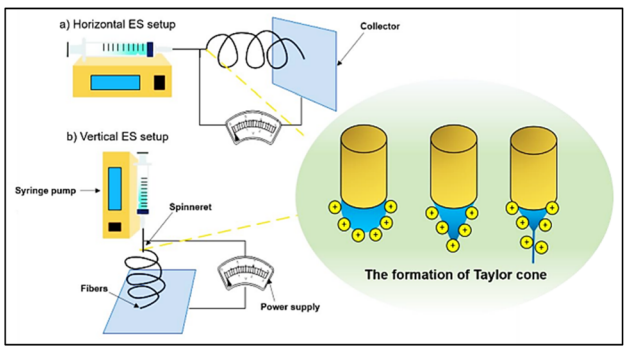

Fig. 6 Setup of the ES system: (a) parallel (horizontal) setup and (b) perpendicular (vertical) setup [Reproduced with permission from ref. 55. A copyright of Elsevier, 2019].

mechanical stability, thermal stability high SSA,[59] and ease of manufacture,[60–62] CNFs have been viewed as one of the most promising options for SCs. Every polymer with a carbon chain can be used as an ES CNF starting material, and they can be classified into water-soluble polymers, like poly-vinyl pyrrolidone (PVP), polyvinyl acetate (PVAc), polyvinyl alcohol (PVA), and poly-ethylene oxide (PEO), and water-insoluble polymers, including polyvinylidene fluoride (PVDF), and polyacrylonitrile (PAN).[63–67] Nonetheless, PAN was found to be the most often used ES carbon NF precursor due to its excellent characteristics, particularly large carbon output (more than 50%), flexibility, and environmental well-being.[68–70]

CNFs can be created mainly within two phases, starting with stabilization and ending with carbonization. To stabilize the ES NFs, they are first put in a tube furnace and heated between 250 and 300 °C. The polymer is now transformed into a compound with a double-stranded polymer with the connectivity of a ladder, which aids in maintaining the fibrous structural morphology at elevated temperatures. The stabilized fibers are next turned into CNFs that resemble graphite by carbonization in an inactive environment at a temperature exceeding 505 °C, as seen in Fig. 7. Fig. 7 shows the variation in structural morphology of poly-acrylonitrile (PAN) to CNFs. Additionally, the majority of non-carbon components (H_2O, NH_3, HCN, CO_2, N_2, and CO) are removed along this procedure,[71] which reduces the diameter dimensions of CNFs and increases accessible surface area and hence conductivity also gets increased. Furthermore, the creation of a porous structural morphology in CNFs, *i.e.*, microporous (<2 nm in size), mesoporous (2–50 nm), and macroporous (>50 nm) has been extensively researched for flexible SCs (FSCs). Feng and his team observed that microporous CNFs (2.0 nm) can boost charge transfer resistance because they partially stop electrolytes from entering the microporous electrode, even during charging/discharging.[72] As they have higher electrochemical performance, mesoporous (2.0–50 nm) CNFs are favorable to alleviate this ionic diffusion.[73,74] Intriguingly, micro/mesoporous CNFs produced from PAN-based fibers, a silica pattern, and potassium hydroxide treatment have SSAs up to 1796 $m^2\ g^{-1}$, which promotes the quick passage and diffusion of electroactive species while displaying a large electrical capacity of 198 F g^{-1}.[75] Although their capacitance has grown, a study has been done to control the void size within porous CNFs for better electrochemical performance in SCs.[76]

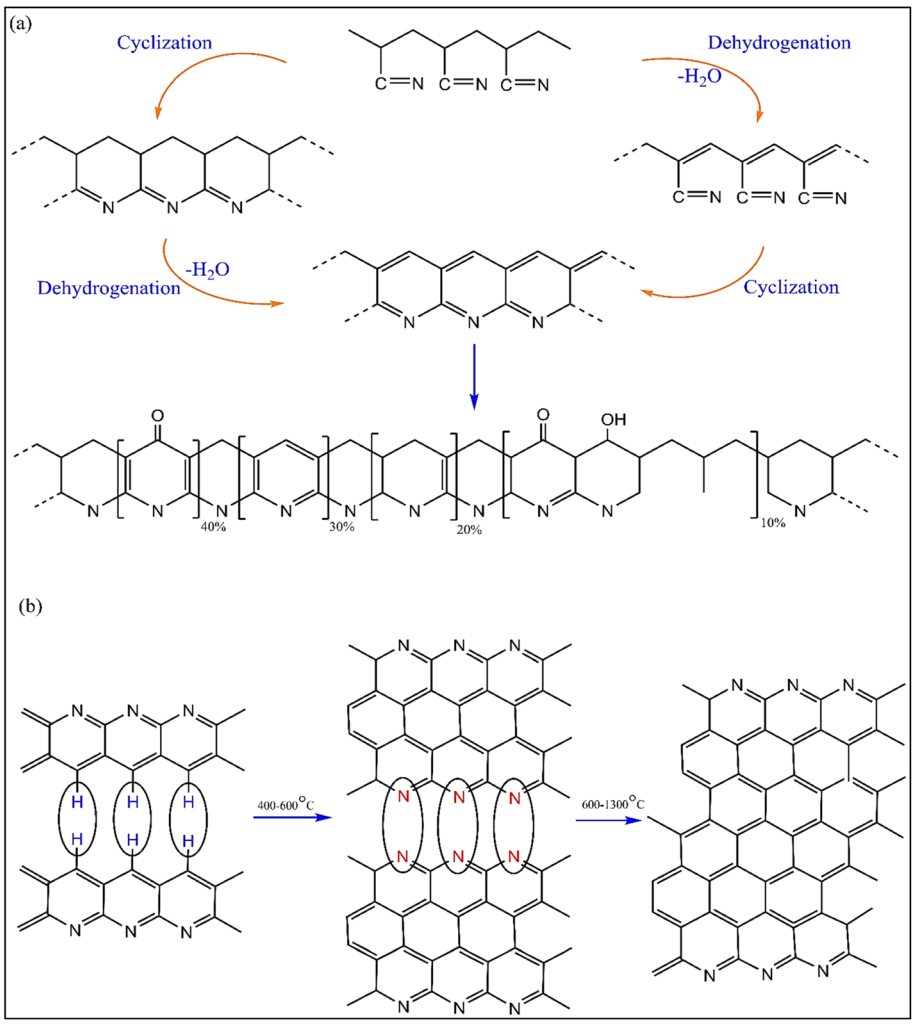

Fig. 7 Variation in the structural morphology of poly-acrylonitrile (PAN) to CNFs using (a) stabilization[76] and (b) carbonization[77] methods.

3. Electrode materials

SCs have two properties, specific capacitance, and charge-storage density, which are affected by the composition of electrode materials used.

3.1. Carbon materials

All types of carbon compounds are used as electrode materials while making SCs. Large surface area, low price, accessibility, and well-established electrode production technology are the few reasons for using C-based materials in SCs.[78] C-based materials use an electrochemical DL storage system, which forms at the electrolyte/electrode interface. Thus, the capacitance mostly depends on the area of the surface where electrolyte ions come into contact with the electrode. Electrochemical performance is significantly influenced by SSA, pore structure, shape and size distribution of pores, functional groups at the surface, and electrical properties.[79–81] In particular, when it comes to carbon materials, they have large SSA, which enhances the capacity for the charge to build up at the electrode–electrolyte contact. When boosting specific capacitance for carbon materials, surface functionalization must take into consideration the pore size and large SSA. A few examples of carbon compounds used in fabricating the electrode materials of SCs include charcoal filters, carbon aerogels, CNTs, graphene, and other forms of carbon.

3.1.1. Activated carbon (AC) based SCs. AC has a large SSA, robust electrical conductivity, and a competitive price.[82] It is possible to produce AC by physically or chemically activating some carbon-related materials (for example, coal, nutshell, wood, *etc.*). The carbon precursors must be heated to a high temperature (between 750 and 1150 °C) to be physically activated. Chemical activation does not require high temperatures and is done by using activators including $ZnCl_2$, NaOH, KOH, and H_3PO_4.[83] AC provides a well-defined surface area of 3000 m^2 g^{-1} and a diversity in physicochemical properties. There are a variety of pore sizes in the AC produced by activation, comprising macro-pores (>50.0 nm), mesopores (>2.0 nm), and micro-pores (~2.0 nm).[84,85]

Different studies have assessed this connection, and there appears to be an imbalance between specific capacitance and a particular surface area of AC. A comparatively low capacitance was achieved with a high SSA of around 3000 m^2 g^{-1}.[86] This demonstrates that not all pores are productive while charges are accumulating. Therefore, even if the SSA in EDLC is a key performance parameter, other factors are also taken into account in carbon materials, such as pore size distribution, which has a significant impact on electrochemical performance.[87] Moreover, over-activation results in a high pore volume, which has limitations, *i.e.*, small conductivity and density, which causes low EDs and a decrease in power capacity.

An attempt was made to ascertain how different electrolytes affect the functionality of AC in affecting the capacitance of SCs. It was found that aqueous electrolytes present between AC-based electrodes have a higher capacitance (ranging from 100 F g^{-1} to 300 F g^{-1}) than organic electrolytes (150 F g^{-1}).[88] Cooked chicken bone waste along with KOH electrolyte was used as an electrode material for SCs. The chicken bone-based SCs show a specific energy of 11.3 W h kg^{-1} and a specific power of 8.50 kW kg^{-1}.[89]

3.1.2. CNT-based SCs. The study of carbon materials has significantly grown since the discovery of CNTs in both science and engineering. The total component resistance of SCs is what defines their power density. CNTs have received a considerable amount of attention as SC electrode materials because of their unique pore structure, great mechanical and thermal stability, and extraordinary electrical conductivity.[90,91] Certain hydrocarbons require catalytic breakdown to produce CNTs. It is possible to make nanostructures in a range of conformations and have control over their crystalline structure by carefully adjusting some factors.[92] Because the mesopores in CNTs are linked, unlike those in other carbon-based electrodes, this enables a continuous charge distribution that practically uses the whole available surface area. Since the electrolyte may infiltrate into the mesoporous network, CNTs have a smaller Equivalent Series Resistance (ESR) than AC.[93] SWCNTs and MWCNTs are the two varieties of CNTs being researched as prominent materials for SC electrodes.[94] The strong electrical conduction and easily accessible surface area of CNTs make them recognized as high-power electrode materials. They also form an excellent basis for active nanomaterials owing to their excellent mechanical durability and tubular structure.

As opposed to AC, CNTs often have a tiny SSA (500 m^2 g^{-1} or less), which results in lower EDs. To increase CNT's specific capacitance, KOH can be chemically used as an activator. The aforementioned technique can significantly enhance CNTs' surface area (by a two- to three-fold factor) while preserving their nano-tubular architecture.[83]

CNTs have been extensively investigated as electrode materials for SCs due to their unique properties, including high surface area, excellent electrical conductivity, and mechanical strength. To increase the performance of CNT-based SCs, researchers have developed NCs by incorporating CNTs with other materials. Here are some examples of NCs used as electrode materials in CNT-based SCs: (i) CNTs/MO NCs: MOs such as MnO_2, RuO_2, and NiO have been combined with CNTs to form NC-based electrode materials of SCs.[88–94] These materials provide additional pseudocapacitance, which significantly increases the energy storage capacity of SCs. The combination of CNTs with MO can be achieved through various methods, including electrodeposition, CVD, or hydrothermal synthesis, (ii) CNTs/CPs NCs: CPs, such as PPy, PANI, and poly(3,4-ethylene dioxythiophene), have been integrated with CNTs to create NC based electrode materials of SCs. The CPs contribute to the overall capacitance of the SCs, while CNTs provide enhanced electrical conductivity and mechanical stability. These NCs can be synthesized through methods such as *in situ* polymerization or electrochemical deposition, (iii) CNTs/graphene NCs: graphene, another carbon-based material, has been combined with CNTs to form NC-based electrode materials of SCs. The combination of these two-dimensional carbon materials offers a large surface area, high electrical conductivity, and excellent mechanical properties. The NC structure facilitates charge transfer and improves the overall performance

of the SCs, and (iv) CNTs/metal NCs: metal NPs, such as Au, Ag, and Pt, have been incorporated into CNTs to fabricate NCs. The presence of metal NPs enhances the electrochemical activity of the electrode, leading to increased energy storage capacity. The synthesis of CNTs/metal NCs can be achieved through methods such as chemical reduction or electrodeposition. The specific choice of NC-based electrode materials in SCs depends on the desired properties and performance requirements of the SCs.

3.1.3. Graphene-based SCs. Graphene has received a lot of interest recently.[95,96] Graphene is a unique carbon derivative that has the potential to be used in ESD applications due to its exceptional properties of appreciable conductivity, chemical stability, and broad surface for adsorption and catalytic reactions.[97–100] The use of graphene as a material for SC applications has recently been proposed because, unlike many other carbon materials like AC and CNTs, graphene's usage as an electrode material for SCs does not depend on the dispersion of pores in the solid state.[100,101] The SSA of newly synthesized graphene, which is about 2630 $m^2 g^{-1}$, is larger than that of any other carbon-based nanomaterials used in the fabrication of electrodes in EDLCs.[102,103] If the full potential of the SSA is used, graphene can achieve a capacitance of up to 550 F g^{-1}.[97]

CVD, arc discharge, micro-mechanical exfoliation,[104] unfolding CNTs, chemical and electrochemical processes, and intercalation of carbon–graphite are just a few of the procedures that may be used to produce different types of graphene.[105–107] The high intrinsic surface capacitance and SSA of single-layer graphene were utilized in the fabrication of graphene-based electrode materials for SCs. Efforts were made to prevent graphene sheets from stacking on one another during the synthesis of graphene along with electrode production. Blended graphene sheets were developed to achieve high efficiency and prevent face-to-face stacking. An ED of 85.6 W h kg^{-1} was achieved at standard temperature and 136 W h kg^{-1} at 80 °C with the current at 1.0 A g^{-1}. The reported EDs are similar to that of the Ni–H battery.[97] Aqueous and organic electrolytes were investigated with chemically modified graphene (CMG), and electrical capacities up to 135 and 99 F g^{-1} were produced.[4] The results are better than carbon-based SC electrodes. For example, when the potential is 1.0 volt and an aqueous electrolyte is present, the graphene material used in SC electrodes produces a better capacitance of 205 F g^{-1} with an ED of 28.5 W h kg^{-1}. A single-layer graphene oxide (GO) sheet was depleted in the experiment using gas-based hydrazine at ambient temperature. The graphene produced by this method is less agglomerated than graphene manufactured using an aqueous solution-based synthesis of chemically altered graphene.[108] Three distinct approaches were investigated to discover better capacitance by employing graphene as the electrode material for SCs. The first approach used thermally induced graphitic oxide exfoliation, the second involved heating nanodiamonds to a temperature of 1650 °C in a helium environment to produce graphene, and the third involved decomposing camphor over nickel NPs. The graphitic oxide was thermally exfoliated to provide an excellent specific capacity of 118 F g^{-1} and an ED of 32 W h kg^{-1}.[109] It is essential to create SCs with significant capacitance and fast charging at high current densities since high-power applications are the main application of SCs.

A modified Hummers technique and tip sonication method were used to synthesize graphene. Graphene is chemically exfoliated at high temperatures. A novel approach was studied which uses C-precursors to exfoliate graphene owing to unique chemistry taking place at the surface revealed by a low-temperature exfoliation method. The resulting capacitance is greater than that of high-temperature exfoliated graphene.[110,111] The problem of agglomeration and restacking that graphene faces can be minimized in different ways. Graphite oxide was thermally reduced at a high temperature, and then quickly cooled with liquid nitrogen to create sheets of graphene with a high degree of exfoliation. A better specific capacitance of 349 F g^{-1} was achieved. Problems caused by graphene-based electrodes can be improved by using graphene oxide-based NCs.[112]

To conclude, constant efforts are being made to improve the conductivity of SC electrodes by incorporating graphene and its derivatives. Graphene's high electrical conductivity helps in achieving better charge–discharge rates. Attempts were also made towards the development of hybrid materials for hybrid structure electrodes by combining graphene with other materials, such as MO or CPs, which have been explored to optimize energy storage and increase specific capacitance. CNTs are often used in composite electrode materials when used with other materials to increase SC performance. CNT–CP composites, CNT–MO composites, and CNT–graphene composites have been tested for improving the conductivity and capacitance of SCs.

Techniques for aligning CNTs in the electrode structure were developed to maximize the utilization of CNTs' unique properties, such as their high aspect ratio. Porous structures of AC were also utilized towards the development of hybrid electrode materials for SCs. Researchers are focusing on tailoring the pore structure of AC to optimize ion transport and increase surface area. Hierarchically structured AC with micro, meso, and macro-pores has been thoroughly investigated.

New methods of chemical activation have been explored to create AC with improved performance characteristics, such as higher specific capacitance and better charge–discharge rates. Additional manufacturing techniques, such as 3D printing, have been applied to create complex electrode structures with improved performance and design flexibility. Advances in nanomaterial synthesis and integration techniques have enabled the development of electrodes with precisely controlled nanoscale features, leading to enhanced performance.

The use of ionic liquids as advanced electrolytes has gained attention for improving the ED and stability of SCs. Researchers have also explored the use of pseudo-capacitive electrolytes to increase the overall capacitance and ED of SCs. Researchers continue to work on increasing the ED of SCs to bridge the gap between traditional SCs and batteries. Efforts are also being made to enhance the durability and long-term stability of SCs for various applications.

3.2. MO NF-based SCs

MO-NFs have received great attention for usage as PC electrodes in the development of novel high-performance ESDs due to their better specific energy when compared to EDLCs.[113,114]

Certain MO-NFs, such as Co_3O_4, RuO_2, V_2O_5, MnO_2, and NiO, are frequently employed in SCs due to their high specific capacitance.[115–120] Few important MO-NF-based SCs include RuO NFs, MnO NFs, NiO NFs, CoO NFs, CoO NFs, and VO NFs.

MO NPs are often employed as electrode materials in SCs due to their unique properties, which make them suitable for energy storage applications. The electrochemical reactions in SCs involve the storage of electrical energy through the reversible adsorption and desorption of ions at the electrode–electrolyte interface.[113–115] These MO NPs participate in the electrode reactions in different ways. (i) MO NPs have a high surface area and are characterized by a large number of active sites. The high surface area is crucial for enhancing the electrode–electrolyte interface, promoting more significant ion adsorption, and thereby increasing the capacitance of the SCs.[116] (ii) During the charging process, MO NPs undergo oxidation, and metal ions within the oxide matrix release electrons. Simultaneously, cations from the electrolyte, typically in the form of an electrolyte solution, are adsorbed onto the surface of the MO NPs. This process is reversible during the discharge cycle. (iii) SCs operate based on two main mechanisms: double-layer capacitance and pseudocapacitance. MO NPs contribute to both. (iv) Double-layer capacitance can occur at the interface between the electrode and the electrolyte. The high surface area of MO NPs facilitates the formation of an electric double layer, where charged ions are attracted to the charged surface of the NPs.[117] (v) Some MO, especially transition MO like RuO or MnO, exhibit pseudocapacitance. This involves fast and reversible faradaic redox reactions at the surface of the metal oxide nanoparticles. The MO NPs store charge through the reversible electrochemical reaction of the metal ions with the electrolyte.[118] (vi) The stability of MO NPs during repeated charge/discharge cycles is essential for the longevity of the SCs. Some metal oxides may undergo structural changes during cycling, affecting their performance over time. Researchers often focus on designing MO NP structures that can withstand numerous cycles without significant degradation.[119]

MO NPs in SC electrodes participate in electrochemical reactions by providing a high surface area for ion adsorption, promoting double-layer capacitance, and, in some cases, contributing to pseudocapacitance through reversible faradaic redox reactions. The specific properties of the MO and the electrode design play a crucial role in determining the performance characteristics of the SCs.

3.2.1. Ru–O NF-based SCs. RuO_2 is considered a critical electrode material for oxide-based SCs with remarkable capacitive properties due to its high theoretical specific capacitance (between 750 and 1200 F g^{-1}), higher electrical conductivity, and increased rate capability. RuO_2 is regarded as a prospective SC material that is more expensive to prepare than EDLCs and other electrodes based on CPs and has a higher specific energy (7.5 W h kg^{-1}). $RuO_2 \cdot xH_2O$ nanotube electrode SCs were designed with a specific power of 4320 kW kg^{-1} and a specific energy of 7.5 W h kg^{-1}.[121] The clustering of RuO_2 NPs during the charge/discharge process, however, limits RuO_2's higher electrochemical performance.[122] The RuO_2 was electroplated into nano-porous gold, which increased the ionic conductivity and hence increased its capacitance to 1500 F g^{-1}. The efficiency of RuO_2 might be improved by including 1D nanostructures like CNFs, which provide a significant SSA, intense electric conductivity, and mechanical stability.[123] This would make it possible for the composite to propagate charges more effectively. Using CVD and subsequently following RuO_x electrodeposition, Jhao *et al.* produced coaxial NPs of RuO_x and Graphene NFs (GNFs).[124] The created RuO_x/GNF coaxial nanostructures with a macroporous structure enable the excellent spatial and temporal capacity of 53.82 mF cm^{-2} at 50 mV s^{-1} with better periodic stability (84% capacity) across 5×10^3 cycles. Fig. 8 shows the steps for the production of double-walled CNFs modified with RuO_2 and poly(benzimidazole).

Two redox peaks in the Cyclic Voltammetry (CV) of RuO_x/GNF were observed as a result of the faradaic behavior of RuO_x, showing appreciable capacitance. By adding a sacrificial material that will degrade throughout the carbonization process, one can make nano-structured cavities in the carbon polymeric network. Kim *et al.*[125] described the ES of two copolymers, poly methyl methacrylate (PMMA), and polyacrylonitrile (PAN), accompanied by a chemical activation method, to produce RuO_2 and high-mesopore-activated CNFs that is RuPM-ACNFs. The optimum PAN@PMMA mix ratio (70 : 30) produced the largest energy output of 24 W h kg^{-1} at a power rate of 410 W kg^{-1} with a small semi-circle ($R_{ct} = 1.07$), which was mostly due to the presence of mesoporous RuPM that may operate as binding sites for rapid ion transportation. A lot of interest has also arisen in ternary hybrid composites based on RuO_2 for application in high-performance SCs.

Balan and his coworkers[126] used double-walled CNFs of RuO_2 poly-benzimidazole (PBI), abbreviated as CNFs-RuO_2-PBI (RP) composite, to achieve a better maximum specific capacitance of 1060 F g^{-1} when the scan rate was 20 mV s^{-1} over a voltage of 1.3 V for RP-1 (Fig. 9). Fig. 9 shows the design for the preparation of the MnO_2/PCNFs composite, and (b) SEM of the MnO_2/PCNFs composite. By applying a modified polyol technique to embed RuO_2 NPs on functionalized porous CNFs (F-CNFs), this ternary hybrid electrode was developed. In the next step, phosphoric-acid-doped PBI was tested. The RuO_2 NPs were evenly covered with a very thin layer of H_3PO_4 doped PBI without aggregation, as seen in the TEM pictures (Fig. 10). As a result, the resistance caused by charge transport at the electrode–electrolyte interface was decreased. However, creating a ternary composite electrode material requires a lot of time and effort, thus being inappropriate for mass production. As a result, Kim *et al.*[125] suggested ES and activation as a quick and easy way to prepare RuO_2/ACNF. It's interesting to note that the electrode that was already constructed (20% RuO_2 concentration) had a better electrical conductivity (4.8 S cm^{-1}) and a big SSA (678 m^2 g^{-1}), which produced an excellent electrical capacity of 535 F g^{-1} corresponding to 22 mV s^{-1} scans per seconds.

3.2.2. Mn–O NF-based SCs. Due to its better conceptual specific capacity (1375 F g^{-1}), prolonged operational potential, cost-effectiveness, and outstanding environmental compatibility, MnO_2 has been promoted as an ideal material for a faradaic mechanism that may be utilized as another transition MO (replacing RuO_2)[127–130] and to use MnO_2 as an electrode material,

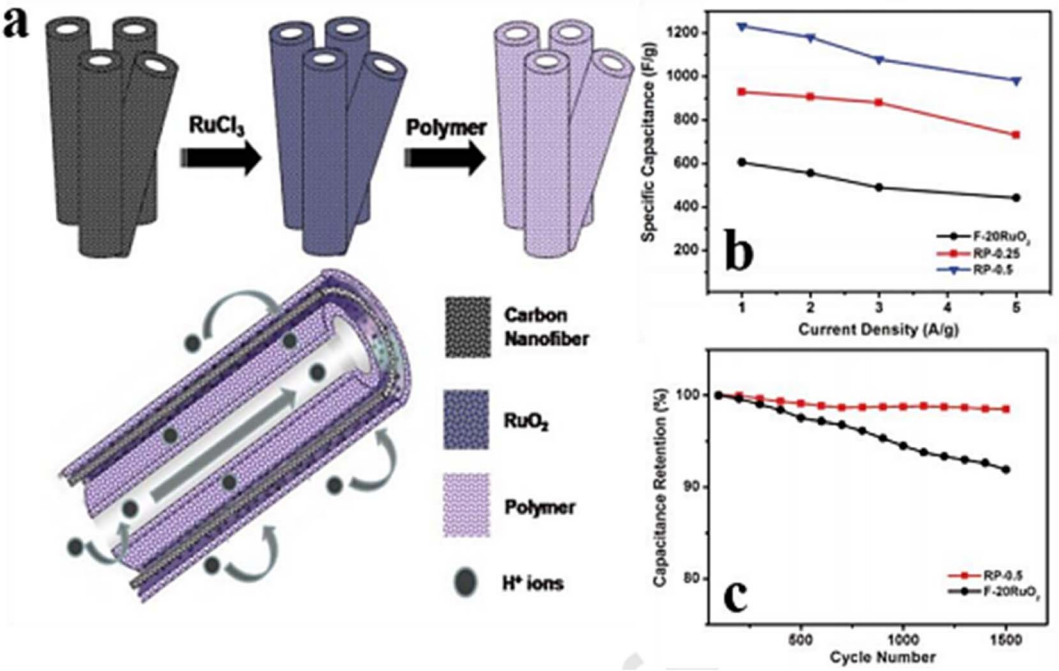

Fig. 8 (a) Steps for the production of double-walled CNFs modified with ruthenium dioxide and poly(benzimidazole). (b) Specific capacitance of F-20 RuO_2, RP-0.25, and RP-0.5 at different current densities from 1.0 to 5.0 A g^{-1}, and (c) electrochemical action of the materials RP-(0.5) and F-(20) RuO_2 in terms of stability for 1500 cycles when the amount of current is 1.0 A g^{-1}.[125] [Reproduced with permission from ref. 125. A copyright of RSC, 2013].

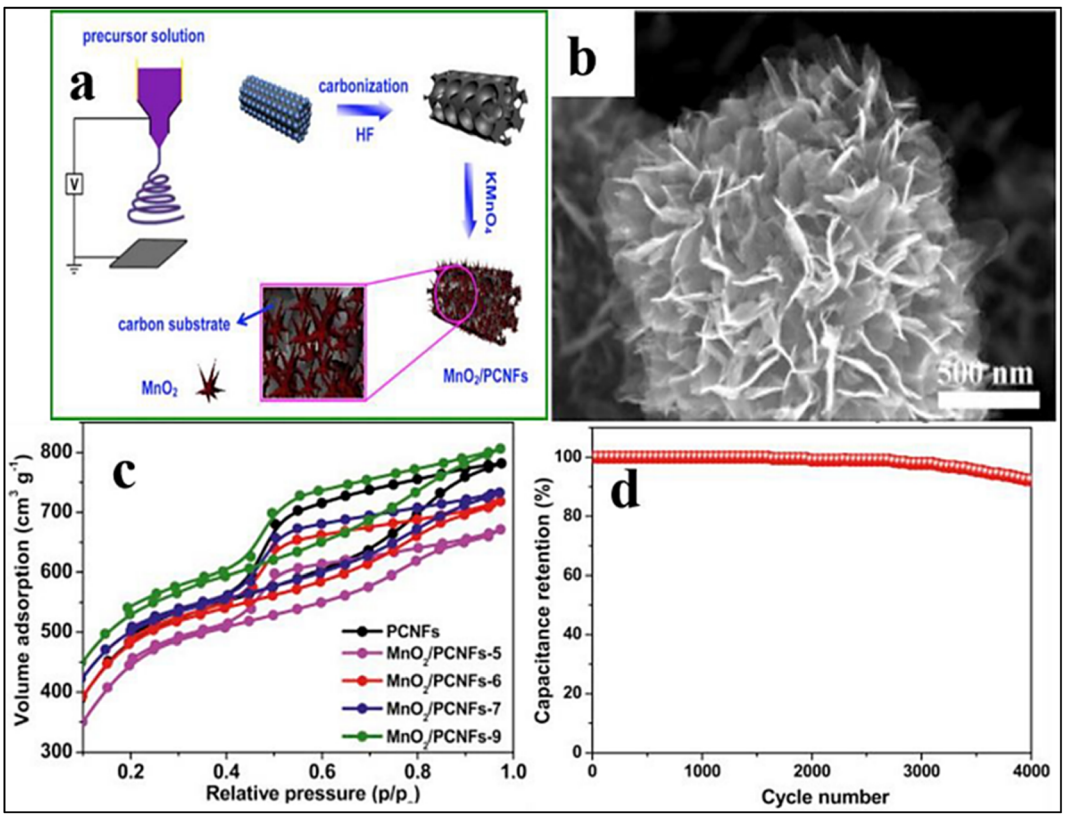

Fig. 9 (A) Design for the preparation of the MnO_2/PCNF composite, (b) SEM of the MnO_2/PCNF composite, (c) isotherm for nitrogen adsorption and desorption of PCNFs and MnO_2/PCNF composite, and (d) cycling stability of MnO_2/PCNFs as an electrode over 4.0×10^3 cycles at a current of 0.5 A g^{-1} [Reproduced with permission from ref. 55. A copyright of Elsevier, 2019].

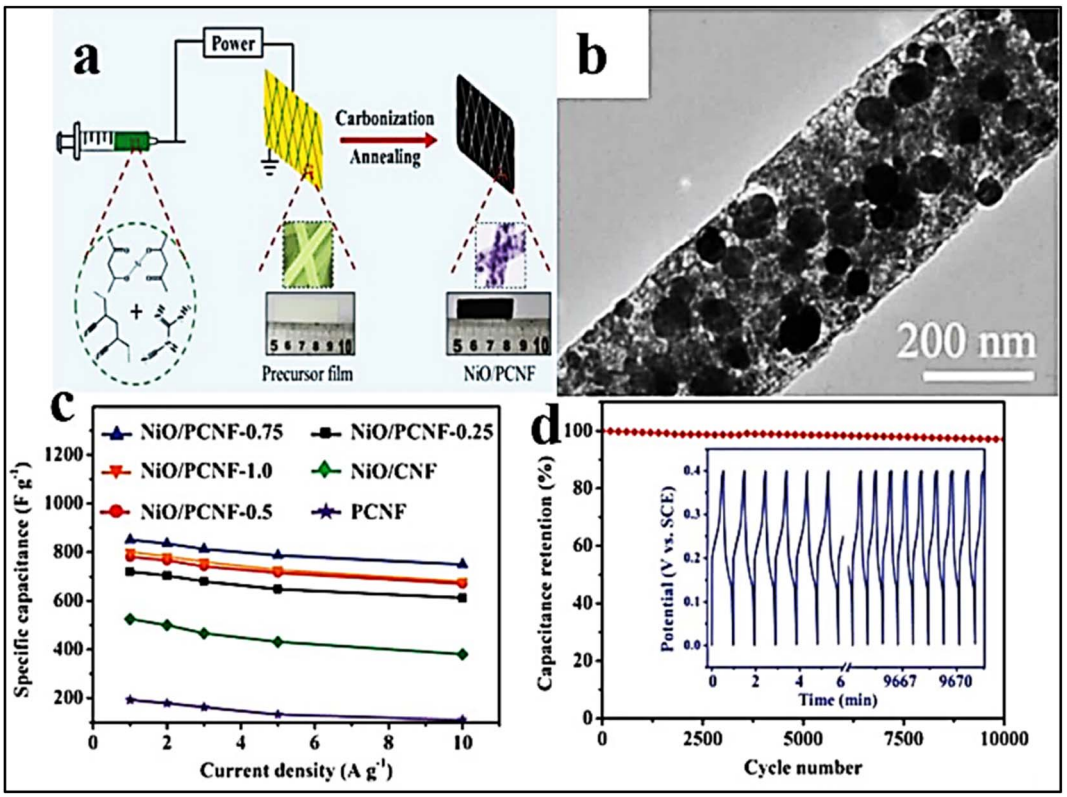

Fig. 10 (a) Fabrication process of the composite made of NiO and PCNF, (b) TEM surface morphology of NiO/PCNF-(0.75), (c) electrical capacity of NiO/PCNF at a composition of 0.25, 0.5, 0.75, and 1.0 against current density (A g^{-1}), and (d) NiO/PCNF-(0.75) cycling stability at a 10 A g^{-1} for 10 000 cycles [Reproduced with permission from ref. 157. A copyright of Wiley, 2018].

one has to understand the mechanism of action of MnO_2 in aqueous electrolytes.[131] A 3D Mn_2O_3@CNT-based electrode material was fabricated with a maximum specific capacity of 868 mA h g^{-1} at 0.2 A g^{-1}.[129] The weak electrical (10^{-5}–10^{-6} S cm^{-1}) and ionic (10^{-13} S cm^{-1}) conductivities[132] of MnO_2 are the sole factors that prevent it from being used in commercial applications and limit its ability to have a useful capacitance and rate. So far, it has been thought that the logical model of MnO_2 nano structural morphologies offers a viable means of using the vast acceptable surface area of fiber materials, which is the conductive and pseudo capacitive nature of MnO_2. Yue *et al.* proposed a metal–organic network made of Mn and Zn as starting materials, and tri-mesic acid (H_3BTC) (Mn-ZnBTC) was pyrolyzed to produce a very thin CNF with the MnO_x–CNFs composite.[135] An electrical capacitance of 180 F g^{-1} was achieved by the non-aggregated, evenly distributed morphology of the MnO_x–CNFs, which also maintained a high periodic durability of 98% over 5000 cycles. The metal–organic network skeleton formed between MnO_x and CNFs increases the conductivity.[133,134] These outcomes can be attributed to the increased MnO_2 and CNF contact area, which has positive synergistic effects for better electrochemical performance. For high electrochemical performance, MnO_2 core–shell type materials were used as electrodes.[135]

Since the electrolyte ion may permeate through the MnO_2 shell in a short (10 nm) distance, mesoporous MnO_2 core–shells covered on the perpendicular alignment of CNFs (MnO_2/CNFs) may offer a larger capacitive performance of 473 F g^{-1}.[135] Furthermore, Klankowski *et al.*[136] and Wen *et al.*[137] have researched the creation of CNFs using degradable, inexpensive bamboo chopsticks. The created carbon-fiber sheets (CFSs) were electrodeposited with MnO_2 NPs (20–50 nm), which resulted in materials with impressive constant capacitance (376 F g^{-1} at 1.0 A g^{-1}), amazing EDs (11.0 W h kg^{-1} at 530 W h g^{-1}), and better long-term periodic stability (99.4% performance was preserved even after 5000 cycles). The synergistic effects of the faradaic charge storage mechanism of EDLC, the enlarged electro-active sites, and the migration of the electrolyte ion contribute to the outstanding electrochemical activities of CFs/MnO_2. Core–shell fibers have been thoroughly studied to achieve a high electrochemical activity in hybrid SCs.[137] For example, PAN solution and PAN–$Mn(NO_3)_2$–PAN mixture were employed as the core and shell solutions, respectively, when C/MnO_2 NC fibres (C/MnO_x) were synthesized utilizing the core–shell ES technique by Pech and Maensiri.[138] Different MnO_2-based nanostructured materials possess different applications, especially in ESDs. The carbon/MnO_x-based composite SCs show the highest specific capacitance of 213.6 F g^{-1} at 0.5 A g^{-1} current density, energy density of 30 mW h g^{-1}, and power density of 249 mW g^{-1}.[138]

The C/MnO_x hybrid was able to acquire a high SSA, which in turn increased the electrical capacity to 214 F g^{-1} in 6.0 M KOH

by using EDLC and pseudo-capacitance of carbon and MnO_x. Zhou *et al.*[139] used a one-step ES process followed by *in situ* deposition to produce the MnO_2 nanoflakes/porous CNFs (MnO_2/PCNFs) as depicted in Fig. 8. SEM imaging shows that manganese oxide nanoflakes grow vertically, forming a sizable lateral area between manganese oxide and the electrolyte ions on the outermost layer of PCNFs. The MnO_2/PCNF nanoflakes were highly mesoporous and had a high SSA (1815 $m^2\ g^{-1}$), which allowed them to retain their initial capacitance even after 4000 cycles. According to the electrochemical impedance spectroscopy (EIS) experiments,[140] the greater charge resistance of MnO_2/PCNFs compared to PCNFs was caused by the electrode's increased induction of high electronic conductivity. To rationally create hierarchical hollow MnO_2 NFs, Xu *et al.*[141] used the hydrothermal technique. The hollow MnO_2 NFs have an SSA of 195 $m^2\ g^{-1}$ and an average mesopore size that is similar to 4.0 nm, according to Brunauer–Emmett–Teller (BET) measurements, offering a sizable number of active sites for electron transport. Also, they show adequate retention; the electrical capacity of MnO_2 NFs could be maintained between 290 and 214 F g^{-1} when the amount of current per gram was in the range of 1.0 and 10.0 A g^{-1}.

For optimal capacitive nature and reversibility, galvanostatic charge–discharge arcs are fabricated in triangular and uniform shapes. Lately, it has been investigated how dopants like boron, which have a pseudo-capacitive effect, might enhance carbon materials' electrochemical performance. Yang and Kim[142] used a one-step ES and carbonization process to hybridize MnO_2 with boron as a dopant to PAN@pitch based-CNFs (PPBMn). It demonstrates how a huge amount of electroactive spots for redox activities are made possible by the low-impedance electron transport channels found in boron and MnO_2. The PPBMn shows a high ED of 25.67 W h kg^{-1} and a better electrical capacity of 209 F g^{-1}. Chi *et al.* used boron as a dopant in MnO_2 crystallites with a possible bonding with hydrogen, producing a high specific capacity of 365 F g^{-1} at a scan rate of 2 mV s^{-1}, which is much greater than that of electrodes that are not doped (306 F g^{-1}).[143]

Furthermore, the interior structure of boron-doped MnO_2 contains Mn^{2+}, which results in low cycling stability (80.5% after 9000 cycles). The combined usage of materials in EDLC with NFs based on MnO_2 overcomes the drawbacks of pseudo-capacitive materials. Encouraging high electrical conductivity, it boosts the number of electroactive locations for immediate ion diffusion. Lee and Kim used ES and thermal processing to generate SCs utilizing MnO_2/HPCNFs/G (MnO_2/hierarchical porous CNFs/graphene).[144] As evidenced by the exceptional electrochemical properties, the HPCNFs/consistent graphitic MnO_2 pattern, which might lower the charge transport barrier, is strongly supported in this category by the strong rate capability attributes and high specific power of graphene. Even at high scan speeds (10–100 mV s^{-1}), MnO_2/HPCNFs/G retained the quasi-rectangular CV shape, resulting in an improved consistent capacitance of 212 F g^{-1} and strong electrochemical reversibility. Lee *et al.* have fabricated MnO_2/porpus carbon fibre and graphene based composite electrode material for SCs.[144] The SCs electrode with a concentration of 5 wt. percent graphene gives a better specific capacitance (210 F g^{-1}), good rate capability, and high energy density (24 W h kg^{-1}) in an electrolyte of 6.0 M KOH solution.

According to Śliwak and Grygleweicz, the counter electrode should be a high voltage non-symmetric SC based on AC, and the positive electrode should be MnO_2/oxidized CNFs.[145] They demonstrated high-efficiency and stable performance (94%) after 5000 cycles when the electrical power was at 100 W kg^{-1} with an ED of 25 W h kg^{-1} in the potential range 0–2.2 V. After 1.0×10^3 charge/discharge cycles at 2.0 V, the efficiency is still above 97% when the positive electrode is formed of reduced graphene oxide (rGO) CNFs and Mn_2CO_3, and the negative electrode is likewise comprised of rGO in 1.0 M Na_2SO_4. δ-MnO_2 NFs and SWCNTs were produced by Wang *et al.* utilizing vacuum filtering.[146] The real capacitance rose to 965 mF cm^{-2}, which is greater than that of SWCNTs and δ-MnO_2 films when used with PVA and KOH as the electrolytes. The findings explain why SWCNTs are superior to other materials. They also help to explain why δ-MnO_2/SWCNT hybrid electrodes have enlarged surface area and an improved electrical conductivity of up to 81.2 S cm^{-1} (Fig. 9).

3.2.3. Ni–O-based NFs used in SCs. In SCs, NiO is treated as one of the most hopeful electrodes due to its large surface area,[148] non-toxicity, and affordable production.[149] Nanoflakes,[153] nanosheets,[151] nanowires,[152] and nanoribbons[150] are some of the important morphologies of NiO. NiO-based NFs can be produced using a variety of methods, including solvothermal, hydrothermal, and chemical immersion. Through the hydrothermal and post-annealing treatments (590 °C), Zhu *et al.* created 3D NiO nanowalls, which helped the CVD procedure to produce CNFs more quickly on metal wires.[153] This method enhances the surface area of NCs, which raises the real capacitance to 12.6 mF cm^{-2} with an impressive efficiency (92%) even after 3000 cycles. By operating a light-emitting diode with two of the capacitors linked in series, the high efficiency of the CNFs/MW 3D NiO SCs was confirmed. The outcome demonstrates a variety of uses for beneficial and portable electronic devices.

Yang *et al.* proposed the direct thermal decomposition of Metal–Organic Frameworks (MOFs) consisting of Ni and Zn for the *in situ* production of diluted NiO–CNFs.[147] The covalent bonding of organic molecules and metal ions in MOFs improves the electrochemical properties and the final product's porosity.[155] Only 28% of the specific capacitance was depleted from its starting capacitance even at high scan rates, because of the mesoporous structure of NiO/CNFs MOFs. This results in a good rate capability of SCs. Moreover, a significant quantity of NiO was distributed across the surface of CNFs, increasing the energy output of SCs to 33.5 W h kg^{-1} with outstanding rate capability and minimal internal resistance. The potential drop observed was small throughout the system.

Zhang *et al.* used NiO sheets to make hollow tube NFs using the ES process using citric acid.[148] Because of their larger surface area and potential electrocapacitive properties, the NCs synthesized from NiO/citric acid exhibit high electrical capacity, *i.e.*, 338 F g^{-1} compared with NiO alone. Furthermore, due to the short electron diffusion paths produced by the development

of a hollow structure, a minimal charge transfer resistance was observed, *i.e.*, 0.25 Ω. NiO has a very low intrinsic conductivity, which is considered a drawback that is rectified by synthesizing a porous NiO/citric acid structure to enhance the reactive surface area. Wang *et al.* have reported metal organic framework based 3D nanostructures for hybrid supercapacitors.[154]

Zang *et al.* have synthesized NiO NFs using a hydrothermal method followed by calcination. Because of their unique surface morphology and quick electron transport during the faradaic process, they showed a capacitive performance of 885 F g^{-1} with 12% capacitance fading even after 1000 cycles.[155] Kundu and Liu[156] developed an easy method to speed up the formation of porous NiO NFs on a nickel foam by the ES process. This simple process yields a 738 F g^{-1} specific capacitance and exceptional stability performance even after 8000 cycles. With the help of active surface sites, the Ni foam was successfully bonded to the porous structure of NiO-NFs, which increased the rate of ion diffusion and enhanced capacitive performance.

Li *et al.* synthesized porous Ni-doped CNFs (PNCNFs) with NiO NPs scattered throughout the framework, which had a better synergistic impact over the NiO NPs and PNCNFs and significantly increased specific capacity to 852 F g^{-1} in 6.0 M KOH electrolyte.[157] Due to the breakdown of dicyandiamide (DCDA), which aids in the uniform dispersion of NiO NPs across the whole framework, different gases (CO, CO_2, H_2O, and NH_3) evolved throughout the entire nano framework. The NiO NPs do not naturally agglomerate. As a result of the creation of pores on the PNCNF surfaces and the presence of non-aggregated NiO, non-breakable charge transport channels may be induced, which improves stability performance by reducing ion diffusion resistance. Additionally, this approach demonstrates that as the Ni concentration on the surface of PCNFs grows, rate capacity improves, leading to an improvement in cycle stability of 97% after 1.0×10^3 cycles (Fig. 10). Fig. 10 shows the fabrication method of NiO and PCNF based electrode materials for SCs. TEM images of electrode materials were shown (Fig. 10b). The variation of specific capacity (F g^{-1}) was observed against current (A g^{-1}) for different types of composite electrodes (Fig. 10c). The specific capacity was found to be higher for the NiO/PCNF-0.75 composite-based electrode material in all current density measurements. The capacity retention power of the NiO/PCNF-0.75 composite-based electrode material was observed after different cycle numbers (Fig. 10d). It was observed that the capacity retention of the NiO/PCNF-0.75 composite-based electrode material was more than 80% even after 10 000 cycles.

3.2.4. Co_3O_4 NF-based SCs. Co_3O_4 has been very recently introduced as the ideal electrode material.[159–164] The improved specific capacitance of Co_3O_4 NF-based SCs was due to its superior redox characteristics.[159,160,239] In comparison to other transition MO, Co_3O_4 is becoming more and more environmentally benign and cost-effective because of the straightforward synthetic process of Co_3O_4 NPs.[161] The surface morphology of the nanomaterials and the electronic structure of metals like Co^{2+} and Co^{3+} typically determine the redox characteristics of Co_3O_4.[162] This guarantees the synthesis of different types of Co_3O_4 NPs with a higher degree of charge transfer capability, which must be employed in fabricating Co_3O_4 NP based SCs. Co_3O_4 NPs and graded porous CNFs were mixed by Yaseen *et al.* to create an HC, which improved its electrical conductivity and stability.[163] This NF hybrid composite was created utilizing the cost-effective ES process, followed by carbonization, which increases ion transport throughout the system and yields a surface area of 485 m^2 g^{-1}.[163] An electrical capacity of 912 F g^{-1} in H_2SO_4 (1.0 M) as the electrolyte was obtained as a consequence of this technique, which exhibits outstanding preservation of initial capacitance after 1000 cycles (approximately 78%). There is an alternative technique to increase the performance's efficacy and stability, which involves employing binary metal oxides, like $CoMnO_2$, in the NC electrodes of SCs.[164]

Utilizing the thermal breakdown of MO and the annealing of vapour-grown CNFs (VGCNFs), Kim *et al.* created Mn/Co binary oxide NFs.[164] VGCNFs have multi-dimensional pathways for electron transfer throughout the system and further minimize the separation between the $CoMnO_2$ electrode and bulky electrolyte. This system produces specific capacitance up to 630 F g^{-1} at a scan rate of 5 mV s^{-1}. When compared to other materials, Ni froth and $CoMnO_2$/VGCNFs demonstrate greater capacitance efficiency, keeping 95% of their original capacitance even after 1.0×10^3 cycles. 1D spinel $CoMnO_2$ porous NFs were also produced at a low cost for solid-state SCs using the one-step ES approach.[165] Additionally, certain holes or gaps that were created in between spherical $CoMnO_2$ particles might serve as an ion buffering resource. This special characteristic of $CoMnO_2$ particles results in a reduced diffusion resistance of up to 6.11 ohm and a good specific energy density of 75 W h kg^{-1} with a power density of 2000 W kg^{-1}.[165]

3.2.5. V_2O_5-NF based SCs. One of the most significant forms of vanadium oxide is V_2O_5, which is thought to be a viable working material for SCs. Because of the variable oxidation states from V^{2+} to V^{5+}, vanadium oxides possess outstanding redox characteristics, a distinctive layered structure,[165] and a large potential window.[166] Recently, NC-based SCs including V_2O_5 and carbonaceous materials like SWCNT, MWCNT, AC, *etc.* have been explored.[166–171] After annealing at 550 °C, Thangappan *et al.* used the ES process to create extremely porous GO/V_2O_5 NFs with a diameter range of roughly 190 to 80 nm.[168] These NCs were unique due to their surface shape, which promotes K^+ diffusion from the electrolyte placed into the pores of NC electrodes. The specific capacity of GO/V_2O_5 increases up to 455 F g^{-1} at 12 mV s^{-1} in a 2.0 M potassium hydroxide electrolyte, which was greater than that of the separate GO and V_2O_5 electrodes. Only a small number of ions may be used by the active electrode in GO/V_2O_5 NFs, and only the activated electrode's outer surface interacts with the NCs during the charging or discharging process. The specific capacity of the NF framework decreases when the scan rate is increased, which is considered a drawback of the GO/V_2O_5 framework.

Utilizing GO with a larger surface area improves capacitance and conductivity, which solves the issue of capacity fading at higher cycles. V_2O_5/CNFs were synthesized by Kim *et al.*[169] utilizing the carbonization and ES techniques. The V_2O_5 utilized in this procedure was used in weight percentages of 5, 10, and 20%. They investigated several V_2O_5 weight percentages to

determine which weight % was best for the CNFC microporous structure. Finally, they concluded that V_2O_5-20 is the material that works well in the microporous structure of CNF–Cs and produces great results, such as specific capacitance up to 152 F g^{-1} and impressive ED of 19 W h kg^{-1} (because of the enlarged area of the region between CNFCs and V_2O_5 (20%)). Multichannel CNFs with amorphous V_2O_5 doped into their microporous structure have been found by Huang *et al.* to provide a higher specific capacity of 745 F g^{-1} with a current density of 0.5 A g^{-1}.[170] An improved relationship between V_2O_5 high capacitance and enlarged surface area can provide SCs with outstanding electrochemical characteristics.

The correlation between V_2O_5 in the multichannel CNF microporous structure increases the region where the electrode and electrolyte interact, which lowers the charge transfer resistance by up to 0.25 Ω. Additionally, due to their numerous oxidation states in the same framework, researchers are currently concentrating on generating mixed transition MO NF composites (binary spinel) to improve specific capacitance and achieve higher efficacy in the stability performance of SCs.[170] For instance, the NCs made from V_2O_5 and Cu_xO (Cu_xO/V_2O_5) by varying the weight fraction of the vanadium and copper precursors exhibit much higher performance and specific capacitance than either Cu_xO or V_2O_5 alone.[171] Large interfacial area in the NCs created from V_2O_5 and Cu_xO precursors reduces charge transfer resistance by 0.2 Ω. Additionally, it increases the charge capacity of bimetallic oxides.[171]

To conclude, different transition MO, including RuO_2, MnO_2, and Co_3O_4, have been extensively studied for their high specific capacitance and electrochemical stability of SCs. Researchers have designed MO NPs with controlled sizes, shapes, and surface structures to optimize their electrochemical properties. NPs with high SSA and porosity are desirable for improving capacitance. Hybrid electrode materials that combine MO NPs with carbonaceous materials, such as graphene, CNTs, or AC, were developed to increase the capacitance and electrical conductivity of SCs. Doping MO NPs with other elements or ions can improve their electrochemical performance. For example, nitrogen-doped MOs can exhibit enhanced capacitance due to the improved electronic conductivity and altered surface chemistry of the composite electrode material of SCs. Atomic layer deposition has been employed to deposit MO NPs with precise control over thickness and uniformity. This technique enables the creation of tailored electrode materials with enhanced electrochemical properties.

Researchers have been working on strategies to increase the ED of SCs using MO NPs. This includes optimizing the design of asymmetric SCs and exploring novel materials for higher voltage operation. Continuous efforts have been made to improve the long-term stability and cycle life of MO-based SCs by mitigating issues like particle aggregation, dissolution, and structural degradation during charge–discharge cycles.

Exploration of alternative MO NPs beyond the commonly studied ones, such as V_2O_5, WO_3, and NiO, for their potential in SC applications is essentially required. Sustainable and environmentally friendly synthesis methods for MO NPs have been a focus of research to reduce the environmental impact of SC uses and production. MO-based SCs have been integrated into various electronic and ESDs, such as wearable electronics, energy harvesters, and hybrid energy storage systems.

3.3. CP-based SCs

Particularly in the case of PCs, CPs are regarded as an outstanding electrode material for SCs. At the surface and across the electrode, they exhibit reversible redox behavior that allows them to retain charges. Conjugate double bonds with free electrons that are delocalized throughout the whole structure are necessary for CPs.[172,173] This gives CPs the ability to conduct heat and electricity. p-Doping or n-doping can increase the conductivity of the polymers. Doping decreases the distance between the conduction band (CB) and the valence band (VB), allowing electrons to travel more freely inside the system in a larger sense; however, this also includes redox polymers containing redox centers, polymeric electrolytes, or polyelectrolytes. Redox polymers and CPs possess different methods for transferring electrons despite having different structural configurations.[174]

For intrinsic CPs, sometimes referred to as ICPs, the conduction process is carried out by the movement of the electronic charge from end-to-end conjugation.[175,176] The hopping process may occur between both the chains, and any flaws if present retard the conduction of electrons.[177] PANI, PPy, polyacetylene (PA), PTh, *etc.* are a few examples of CPs. These CPs are used to make SC electrodes, which have several benefits including strong conductivity, flexibility, affordability, and ease of synthesis. Furthermore, several investigators have observed the electrochemical properties of CPs and their NCs as electrodes and have explored numerous techniques to enhance their characteristics.[178–186] Table 2 shows different types of CPs, their structures, energy gap, and electrical conductivity. CPs are synthesized by the chemical oxidation technique, electrochemical polarization technique, vapor phase polymerization techniques, template polymerization, solid state polymerization, microwave-assisted polymerization, *in situ* polymerization, and many more. Fig. 11 shows different polarization methods for fabricating CP-based electrode materials.

CPs are generally used as electrode materials in SCs due to their unique electrical and electrochemical properties. The diffusion and absorption properties of CPs play a significant role in determining the efficiency of SCs.[180–182] These adsorption and diffusion properties of CPs influence the application of SCs in one or another way. CPs have a porous structure that allows ions from the electrolyte to diffuse and penetrate the bulk of the CPs during the charging and discharging processes. This high ion diffusion capability is crucial for achieving high capacitance and fast charge/discharge rates.[183] CP electrodes usually have a large specific surface area, which enhances the electrode–electrolyte interface and promotes efficient ion diffusion. The higher the surface area, the more ions can be stored, contributing to the overall capacitance of the SCs. CPs can absorb and hold a significant number of electrolytes within their structure. This absorption capacity contributes to the increase in the overall charge storage capacity of the SCs. Some CPs exhibit

Table 2 Different types of CPs, their structures, energy gaps, and electrical conductivity

Types of CPs	Structures	Energy gap (eV)	Conductivity (S cm^{-1})	References
Polyaniline	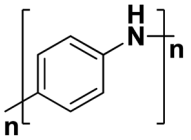	3.2	300–200	180–186
Polypyrrole	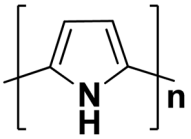	3.1	10^3–1.7×10^5	102–105
Polyacetylene	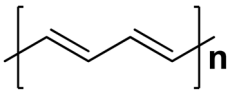	1.5	10^2–1.7×10^3	172–174
Polythiophene	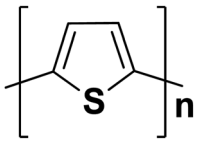	2.0	10×10^3	219–223
Poly(*p*-phenylene vinylene)	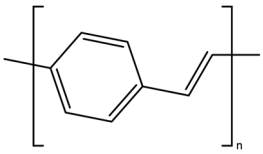	2.5	3.5×10^3	175 and 176
P3HT	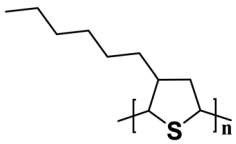	2.3	6.675×10^{-5}–0.34	177
Polyphenylene	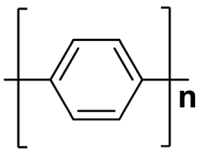	3.0	$10^2 \times 10^3$	17

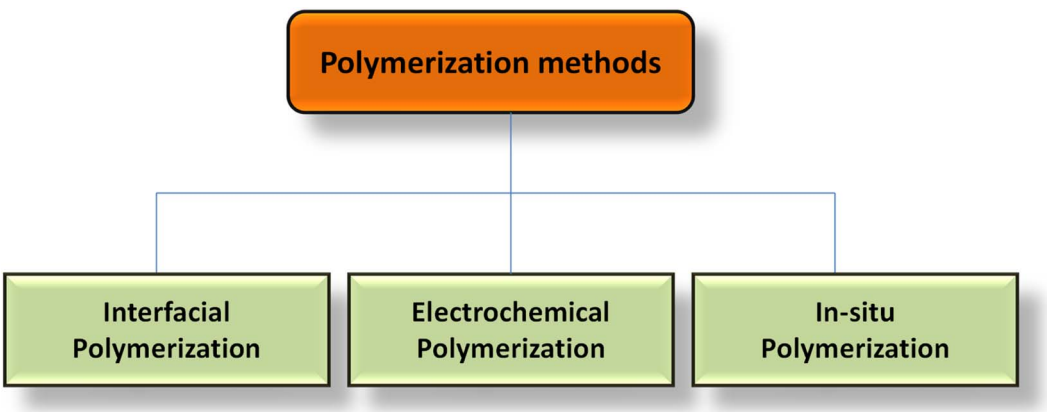

Fig. 11 Different polarization methods for fabricating CP-based electrode materials.

swelling/shrinking behavior during the redox processes associated with charging and discharging. This reversible swelling allows the CPs to accommodate the volume changes associated with ion absorption and desorption, contributing to the longevity and stability of the SCs.[184,185]

The efficient diffusion and absorption properties of CPs contribute to high capacitance values. This means that the SCs can store a large amount of electrical energy per unit mass or volume, making them more efficient in terms of energy storage. The ability of CPs to facilitate rapid ion diffusion allows for fast charge and discharge cycles. This property is crucial for applications where quick bursts of energy are required. The swelling and contraction behavior, combined with the overall structural stability of CPs, influences the cycling stability of the SCs. A stable and reversible redox process, along with minimal structural degradation over numerous cycles, is essential for long-lasting and efficient SCs.[186]

The diffusion and absorption properties of CPs have a significant impact on the efficiency of SCs by influencing key performance factors such as capacitance, charge/discharge rates, and cycling stability. The ability of CPs to effectively accommodate ions and maintain structural stability during repeated cycling contributes to the overall effectiveness and reliability of the SCs.[187–190]

Different synthetic approaches were reported for synthesizing CPs in the current scenario and also had several applications for electrochemical storage devices.[92,179] We will focus on three major CP (PANI, PPy, and PTh) based NCs, their electrochemical properties, and their impact as electrode materials in SCs.

3.3.1. PANI-based SCs. Different techniques were used to polymerize aniline monomer to synthesize PANI, which has benefits including being simple to make and environmentally friendly.[180–182] Sivakumar *et al.* created PANI NFs at a reasonable cost *via* interfacial polymerization techniques.[183] Due to ongoing reversible redox processes that demonstrate a large capacitance of 554 F g^{-1} when a constant current of 1.0 A g^{-1} is applied. The cycle stability was quite poor due to the initial capacitance loss, which was the main drawback. Li *et al.*[184] examined the highest theoretical specific capacity of PANI in sulphuric acid as the electrolyte and discovered a maximum capacity of 608 F g^{-1}. The experimental results are in direct opposition to the values observed by the theoretical technique. This is because a very small amount of PANI contributes to initial capacitance stability after a large number of cycles. In general, using pure PANI as the electrode material in SCs produces improved specific capacitance with a reduction in initial capacitance, which results in a reduction in electrochemical performance efficiency. As a result, researchers concentrated on the synthesis of PANI-based composites by combining PANI with carbon and MO to increase the effectiveness and durability of SCs by increasing their electrochemical characteristics.[184–186]

The electrochemical performance of SCs using the CPs–C composite as the electrode material exhibits a notable increase in efficiency and stability performance of SCs in comparison to individual CP components and CP–carbon material composite. Examples include the PANI/CNTs composite and PANI/CNFs composite, both exhibiting maximum specific capacitance in comparison to the separate components.[191–195] PANI/graphene nanoplate (GN) composites were created by Zhang *et al.*[196] using the *in situ* polymerization process under acidic conditions. SCs having a maximum electrical capacity of 482 F g^{-1} when the amount of current is 0.1 A g^{-1} were produced *via* the associated mechanism. They have great cycling stability efficiency and retain their original capacitance after many cycles. Chemical precipitation was used by Gómez *et al.* to create a PANI/GN composite.[202] The composite made up of PANI and NPs emphasized high-end features and applications.[197] It shows a maximum electrical capacity of 500 F g^{-1} at a current density of 0.1 A g^{-1}. Both examples demonstrate that using a composite CPs–carbon material as an electrode in SCs may increase the specific capacitance of SCs. Furthermore, the NCs made by any CPs, especially PANI and GO, show increased electrochemical activity and greater specific capacity because of the synergetic effect between them.[198–200] The reason why NCs retain their original capacitance to such a great extent is that they offer a far bigger interior surface area than individual components. This characteristic of NCs guarantees increased performance stability and increased efficiency of PANI composite-based electrodes and hence electrochemical characteristics. Additionally, there is little room for improvement in the specific capacitance of carbon materials. Current research thus focuses on modifications in the composite electrode material created by CPs–MO-based SCs.

Researchers recently created a CPs–MO composite, which offered benefits including good cycle stability, excellent conductivity, and a large surface area.[201,202] Gemeay *et al.* discovered that the amount of crystallinity of the NCs PANI/MnO_2 in an acidic medium is influenced by the acidic anions present in the media.[203] Zhang and coworkers created PANI@intercalated multilayer MnO_2 in *N*-methyl-2-pyrrolidone solvent *via* an exchange reaction method.[204] The corresponding process mechanism demonstrates that the composite created had improved conductivity. When the current was 1.0 A g^{-1}, the composite had a maximum electrical capacity of 350 F g^{-1}. Even after 1000 cycles, the composite still had 95% of its initial capacitance. A PANI nanorod-MnO_2 NPs composite film was created by Chen *et al.*[205] When compared to earlier instances and individual components, the NC film created has a significant amount of surface area. As a result, they successfully created electrode materials using the PANI-based NCs, which offer minimum expensive performance which is more effective, good charge storage capability, and are eco-friendly.

3.3.2. PPy-based SCs. In the realm of SCs, PPy is one of the important CPs with a wide variety of uses. Utilizing interfacial polymerization, Yang *et al.* fabricated free-standing PPy films with or without a surfactant.[206] On the PPy surface, tiny holes were created as a result of interfacial polymerization, and the material had outstanding electrochemical performance. They exhibited a maximum electrical capacity of 260 F g^{-1} at 25 mV s^{-1} and preserved over 75% of the original capacitance value even after 1000 cycles. Fig. 12 shows the surface morphology of PPy films produced using the interfacial polymerization technique. Two different surfactants, Tween 80 and Span 80, were used during the

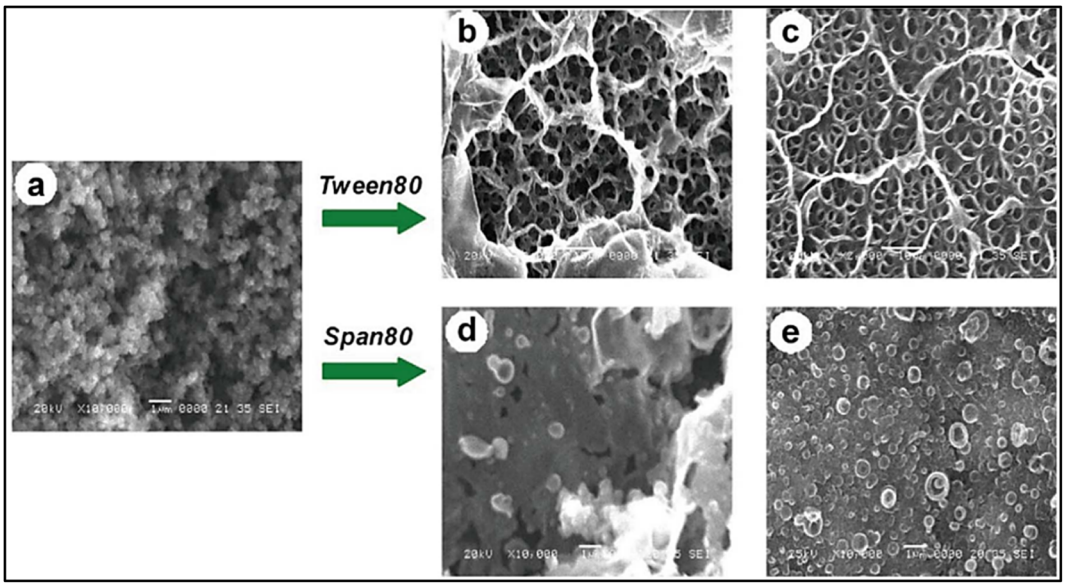

Fig. 12 Surface morphology of PPy films produced using interfacial polymerization technique. (a) PPy fabricated without a surfactant at 25 °C, (b and c) PPy fabricated using Tween 80 and (d and e) PPy fabricated using Span 80 as surfactants at 25 °C and 0 °C [Reproduced with permission from ref. 206. A copyright of Wiley, 2014].

polymerization of PPy CPs. The surface morphology was influenced by the nature of the surfactant used [Fig. 12(c and e)].

Li and Yang[207] used methyl orange/$FeCl_3$ as a reactive, self-destructing template to create a pure PPy film using a chemical oxidation approach. They used 0.5 M $FeCl_3$, and the resulting film was composed of nanotubes of 5 to 6 μm with diameters of 50 to 60 nm. The polymer resulted in significantly better electrochemical performance because of the resulting tube-like structure, which reached a maximum electrical capacity of 578 F g^{-1} at 0.2 A g^{-1}. Even after 1000 cycles in an electrolyte containing 1.0 M KCl, it maintained a capacitance of 80%. Using *in situ* polymerization, Xu *et al.* prepared conductive cotton textiles that were covered with PPy nanorods. The $FeCl_3$-methyl orange complex was used as a template.[208]

Although the fabrics produced by the aforementioned technique have a good specific capacity of 328 F g^{-1} and ED of 25 W h kg^{-1} at a current of 0.7 mA cm^{-2}, they cannot be employed as electrodes for SCs. Although, they can maintain a capacitance of 64% after 500 cycles, their periodical stability is quite low. Rajesh *et al.*[209] created PPy films using phytic acid, a dopant, using the electron polymerization process. As a result, the SC conductivity rises, reaching a maximum electrical capacity of 345 F g^{-1} at a scan rate of 5.0 mV s^{-1}. The preservation of initial capacitance of 90% at 10 A g^{-1} even after 4×10^3 cycles shows that the PPy-based electrode has high specific capacitance.

In general, the synthetic approach, dopant types, template used, and other variables had an impact on the microporous structure and reversible redox characteristics of PPy-based composite electrodes. Even if these parameters are adjusted, some of the qualities of PPy-based composite electrodes can be improved, but other features may deteriorate, making PPy-based electrodes still unable to fulfil the needs of practical applications. Due to the potential for these hybrid composites to improve the energy storage capacity of PPy composites, researchers have recently concentrated on the development of PPy–carbon material composites or PPy–MO NCs.[209–211] Because their reversible redox characteristics have been improved throughout the system, the composites exhibit higher electrochemical performance and better mechanical properties when compared to pure PPy.

Tang *et al.* used the electron deposition approach to create the CNT/PPy film. The CNT/PPy served as the anode in CNTs/MnO_2/KCl@CH_2@CH–SiO_2/poly-acrylamide/CNTs–PPy SCs.[210] When the electron deposition was 2000 s, the specific capacity of these SCs reached a high of 638 F g^{-1} when the amount of current was 1.0 mA cm^{-2}. Additionally, the ED reached a maximum value of roughly 40 W h kg^{-1} having a power of 520 kW kg^{-1} and a strain of 100%, demonstrating greatly increased stability. The composite showed better efficiency in specific capacitance compared with individual components. By using an *in situ* chemical oxidation approach, Yang *et al.* created unique PPy/CNTs composites that are connected in their structure.[211] The conductivity and thermal stability of the associated composites were enhanced when PPy was evenly coated on the surface of air plasma-activated CNTs. Overall, the PPy/plasma-activated CNTs composite's electrochemical characteristics are improved and are higher than those of the PPy/CNTs composite. Additionally, the conjugated structure created at the active sites made available by the nitrogen groups on PPy strengthens the interaction between CNTs. The development of composites with better electrochemical characteristics is facilitated by PPy. By making adjustments to the elements that are essential for the creation of the composite, the mechanical characteristics of the PPy/CNTs composite may also be enhanced. Chen *et al.* synthesized a durable and flexible CNT-based electrode

material for SCs.[212] In this combination, a vacuum-filtered CNT film was covered with PPy that was electronically deposited.

The mechanical qualities of the electrode material are improved by this method, which also increases electrochemical performance. SCs using the aforementioned electrode (PPy/CNT) produced long-term stability and exceptional flexibility, retaining ~95% of their initial capacity even after 1.0×10^4 cycles. However, despite significant improvements in electrochemical efficiency for PPy/CNT composite's cycling stability, these NC electrode materials still have lower energy and power densities than LIBs due to their limited capacity for charge build-up.[212] Due to these factors, SCs using the PPy/CNT composite as their electrode material are unable to satisfy the demands of real-world applications. As the demand for improved electrode materials grows, researchers concentrate on creating composite materials using PPy and metal oxides. High theoretical capacitances are present in MO-based composites.[213] For instance, a PPy/MnO_2 nanowire composite was created by Shayeh *et al.* using an electrochemical oxidation method.[215] Increased specific capacitance due to this process can reach 210 F g^{-1}, almost twice as much as the value of a single PPy (104 F g^{-1}).

Metal oxides are regarded as the optimum active material for PCs, including Co_3O_4,[213] MnO_2,[214] NiO,[216] CuO,[217] WO_3,[218] VO_x,[219] and V_2O_5.[220] Their hypothetical capacitance was more than that of pure PPy. The theoretical capacitance of Co_3O_4 is greater than 3000 F g^{-1}; however, in fact, it was discovered that the experimental capacitance of the corresponding MO is lower than the theoretical value.[213] It is because standard dense electrode films have a restriction on ion diffusion, and low conductivity results in worse electron transport.[221,222] Additionally, they also encounter volume changes as a result of the unstable charge/discharge transfer. Better capacitance is produced by adjusting the charge/discharge process and enhancing conductivity.

Researchers concentrate on creating NCs out of various electroactive materials including CPs and MO since they offer so many benefits. They have good electrical, mechanical, and electrochemical capabilities, resulting in the development of ESDs.[220] 3D NCs made of a PPy@CoO hybrid nanowire array on nickel foam were created by Zhou *et al.* and exhibited good pseudo-capacitive performance.[223] Since it has great rate capability, its specific capacitance reaches a maximum of up to 2225 F g^{-1} at a current of 1.0 mA cm^{-2}, which leads to the retention of an initial specific capacity of 99.7% after 2000 cycles at a scan rate of 20 mA cm^{-2}. It served as a positive electrode in an aqueous asymmetric SC with a hybrid array that can provide EDs of up to 34 W h kg^{-1} as its maximum. It also has a higher power density, which was measured at 5500 W kg^{-1}. The perfect synergetic effect between the PPy and the CoO nanowires is the reason why this SC exhibits exceptional stability for 2000 cycles.

Ji *et al.*[216] created a PPy nanotube/MnO_2 composite using a simple method that exhibits outstanding cyclic stability and specific capacitance of a maximum of 405 F g^{-1} at a current of 1.0 A g^{-1}. Even after 800 cycles, it still retains up to 89% of its original capacitance. The efficiency results from a superior synergistic interaction between PPy and MnO_2, which increases the capacitance. Coated MnO_2 also prevents structural changes in PPy during long-term cycles. Sun *et al.*[221] used a two-step process to synthesize the resulting PPy/V_2O_5, which exhibits greater electrochemical performance efficiency than either component alone. Furthermore, using a direct electrochemical co-deposition process on an interdigital-like electrode, Qian *et al.*[218] created a core/shell CuO/PPy nanosheet array for distinctive on-chip SCs. An exceptional electrical capacity of 1276 F cm^{-3} and an energy per volume of 29 W h cm^{-3} are produced by this process. The device's ability to maintain its specific capacitance up to 100% at a current density of 2.6 A cm^{-3} even after 3000 cycles is its main benefit. The device's strong electrochemical characteristics demonstrate its potential for use in practical SC electrode applications.

In general, electrode materials for SC composites consisting of PPy and MO frequently demonstrate good electrochemical performance, including power density, high EDs, exceptional, superior cycle stability, and amazing specific capacity, due to the synergistic effect of the two composites.[222]

3.3.3. PTh-based SCs. PTh and its derivatives are regarded as superb SC electrode materials and have recently drawn a lot of interest from the scientific community. This is because they have greater environmental stability, higher electrical conductivity, and extended wavelength absorption.[223–225] As a result, research on pure PTh electrode materials has increased, and researchers have concentrated on creating different synthesis techniques for PTh-based SCs.[226] By using a chemical process, Laforgue *et al.* created a pure PTh-based electrode material.[228] This activated material produced a high specific capacitance at a current of 40 mA h g^{-1} and remarkable cycling stability, allowing its original capacitance to be retained even after 500 cycles. Another typical example of this kind is a symmetric SC with flexible and wire-like properties, where the electrode material was made by electrochemically polymerizing PTh and coating a TiO_2 wire, fabricated by Ambade *et al.*[229] This SC device has outstanding cycle stability and a capacitance of 1537 mF g^{-1}. Even after 3000 cycles, it still retains 96% of its initial capacitance.

Gnanakan *et al.* used the dilute polymerization process to create perfect PTh-based NPs and PTh/tartaric acid (TA) NPs in which TA functions as a dopant.[231] These two NPs had a specific capacity of 135 and 157 F g^{-1}, respectively. Nejati used an oxidative chemical vapor deposition approach to make a PTh film without any replacement, which is covered with an ultrathin layer over a variety of substrates.[232] According to the experimental findings, the specific capacity of an activated carbon electrode wrapped using the PTh film rose to 50% when compared to an active carbon electrode that was not coated, and up to 90% of its initial capacity might still be present even after 5.0×10^3 cycles. By using a sequential ionic layer deposition and reaction approach with $FeCl_3$ as the oxidizing agent, Patil *et al.* created an amorphous form of PTh.[233] In 0.1 M $LiClO_4$ metal salt solution, this mechanism produces a capacitance of 255 F g^{-1}.

In general, pure PTh-based electrode materials for SCs are often impacted by a variety of variables, which has an impact on their electrochemical performance. These elements include the surface structure of PTh, the methods used for production, the creation of the substrate, and more. Due to the adjustment of the aforementioned parameters in the recent scenario, the electrochemical performance was significantly enhanced. However, it is still unable

to satisfy the demands of practical applications because its inherent limitations, such as rapid loss of power density and low specific capacitance, make it inferior to PPy and PANI.[233]

Nowadays, researchers are focussing on the fabrication of PTh-based NC materials to address the drawbacks of pure PTh-based electrode materials. To create PTh NCs, there are primarily two types of methods: one involves creating composites of PTh and carbon nanomaterials, and the other involves PTh and MO. A PTh/MWCNTs composite, which may be used as a representative example for the first category, was created by Fu *et al.*[235] The aforementioned electrochemical polymerization process was used to create the PTh NCs. This PTh/MWCNT composite outperforms individual MWCNT and pure PTh in terms of electrochemical performance. At a scan speed of 60 mV s^{-1}, it had a maximum electrical capacity of 110 F g^{-1}. Even after 1000 continuous cycles, the SCs employing the aforementioned PTh/MWCNT composites as the electrodes still retain up to 90% of their initial capacitance. Through the use of an electrochemical polymerization process, Zhang *et al.* created a PTh/MWCNT composite of thickness 2–3 nm.[236] When the amount of current was 1.0 A g^{-1}, this composite then displayed an increasing specific capacity of 218 F g^{-1} because of the insignificant internal resistance, which promoted strong electron transport between the two electrodes of SCs.

Ambade *et al.* gave an easy method to fabricate graphite/thiophene/benzylidene (GTB) and GO/thiophene/benzylidene (GO-TB) using *in situ* polymerization of conjugated polymer PTh (PTCPs).[239] By creating and manufacturing GTB and GO-TB, the PTCP film was non-covalently bound on both the graphene and GO sheets in the NCs, which improves the synergistic impact of the microstructures and also delivers improved doping in graphene. The electrochemical experiments show that the GO-TB composite exhibited better electrochemical performance, resulting in lower serial resistance, excellent specific capacity, and EDs of 298 F g^{-1} and 150 W h kg^{-1}, respectively. It also showed high cycling stability and increased ionic conductivity. Because of the synergistic impact, PTh/carbon material composites demonstrated greater capacitance and cycle stability when compared to single components. Different factors affect the performance of these SCs like the type of PTh, the shape and dimensions of the electrode, production techniques, and efficiency of accumulation of PTh on carbon materials. As previously described for PANI and PPy-based MO composites, PTh-based composites are also appropriate for the production of electrode materials for SCs. Because the specific capacity of SCs with PTh electrodes is substantially less than that of PPy and PANI-based SCs, progress in the development of PTh/MO composites is slower than that of PANI/MO and PPy/MO composites. There is no effective way to enhance the electrochemical performance of CP-based SCs.

Currently, there has been some research performed on PTh/MO composite-based electrodes of SCs.[237,238] To improve the electrochemical performance efficiency, more research is required. The composites formed between the above-mentioned CPs and other materials like activated carbon, CNTs, *etc.* also had merits and demerits.

All three CP and NC-based SCs have merits and demerits. Merits of PANI CPs include a high range of specific capacitance, ease of synthesis, and ease of control of the conductivity. It has high flexibility. Doping and de-doping are simple in the PANI. PANI also shows high theoretical capacitance. The demerit of PANI is that the specific capacitance depends upon the fabrication method. It also shows poor cycling stability. PANI-based electrodes are applied in proton-type electrolytes only.[198–204]

Merits of PPy are high specific capacitance per volume, being easy to synthesize, and have greater cycling stability than PANI. It also shows better flexibility than PANI. It is mainly used to neutralize electrolytes. Demerits of PPy are as follows: doping and de-doping is difficult, it has low specific capacitance per unit gram, and it can be used only as a material for the cathode.[219–222]

PTh has advantages, *i.e.*, it is also flexible, the synthesis technique is much easier, and stability in the environment is very high. The cycling stability of PTh is favorable. Demerits of PTh are that its conductivity, and specific capacitance are very poor.[223–238]

While all three, *i.e.* PANI, PPy, and PTh, CPs-based electrode materials used separately in SCs offer advantages for energy storage applications, there are some differences in their properties and performance. PANI exhibits pseudocapacitive behavior, which means that the charge storage mechanism involves redox reactions at the electrode–electrolyte interface. PANI-based electrodes generally have high specific capacitance and good cycling stability. However, the low intrinsic conductivity of PANI limits its overall energy density and power density compared to other materials. PPy-based electrodes exhibit pseudocapacitive behavior, providing high specific capacitance. PPy has a relatively higher intrinsic conductivity compared to PANI, allowing for better charge transfer and higher power density. However, PPy electrodes may suffer from decreased cycling stability over long-term use due to structural degradation and potential leaching of dopant ions. PTh-based electrodes in SCs exhibit a combination of both EDLC and pseudocapacitance, providing a balanced energy storage mechanism. PTh offers good cycling stability and long-term electrochemical performance. However, compared to PANI and PPy, PTh typically has a lower specific capacitance, limiting its overall energy storage capacity. Overall, the choice of CPs for SCs electrodes depends on the specific requirements of the application. Researchers often explore composite materials and hybrid systems to combine the advantages of different CPs and optimize the overall performance of SCs.

4. Ternary NC, *i.e.*, carbon material/CP/MO-based SCs

In the past, researchers were focused on creating binary NC-based SCs since they attracted more attention due to their superior electrochemical and mechanical capabilities compared to their separate components.[239] In the current scenario, researchers worked hard to develop carbon material-based ternary NCs because the composites show better resultant electrochemical and mechanical properties than CP-based binary NCs.[240] Different factors affect the electrochemical

performance of carbon-based ternary NCs, including synergistic effect, conductivity, surface area, internal resistance, specific capacitance, cycling stability, *etc.* This section discusses the most recent advancements in various carbon-based ternary NCs used as SC electrode materials.

Due to the potential physical and chemical relevance of carbon materials, CPs, and MO, different researchers have attempted to synthesize carbon/CP/MO-based composites.[241,242] A dynamic electrode for SCs was fabricated by Chen *et al.*[242] using a nanowire network of freestanding $NiMoO_4$ that is equally dispersed in all directions. This standalone $NiMoO_4$ nanowire array, which was coated with the CP PANI and a conductive carbon cloth, is recognized as an effective electrode layer for PCs. The final composite showed better electrochemical performance and may be employed as an outstanding electrode in SCs. This indicates improved cycle durability and rate capabilities. A CP/MO electrode material based ternary composite with carbon cloth was prepared through hydrothermal methods and also had application in the field of ESDs.[243] Fig. 13 shows the fabrication process of carbon cloth/PANI/$NiMoO_4$-based flexible electrode materials used in SCs.

In comparison to individual components, the aforementioned NCs have an exceptional specific capacitance of 1340 F g^{-1} at 1.0 mA cm^{-2}, and they preserve their original capacitance of 97% even after 2000 cycles. Dynamic graphene oxide (GO), PPy, and manganese oxide (GO/PPy/MnO_x) NCs were fabricated by Ng *et al.*[245] and used as a working electrode in SCs. They showed strong cycling stability and better specific capacitance even after 1000 cycles and were able to maintain an initial capacitance of 96.5%. Using GO and PPy, MOs like TiO_2 (ref. 246) and ZnO[247] different ternary electrode materials for SCs were also tested. Using GO, ternary composites demonstrated good electrochemical and mechanical characteristics.

Sk's team developed the MWCNT/MnO_2/PANI ternary NCs using *in situ* polymerization. They reported a unique MWCNT-based composite electrode material with pseudo capacitance.[243] The specific capacitance of these NCs can reach a maximum of 530 F g^{-1} and EDs can reach a maximum of 74 W h kg^{-1}, while the π–π interactions, and n–π interactions between constituents improve the electrochemical performance. The power density reached as high as 11.35 kW kg^{-1}. A pseudo-capacitive shell was produced after evenly coating CNT with MnO_2. The resulting NC working electrode produces increased capacitive performance up to a maximum value of 529.5 F g^{-1} at 0.1 A g^{-1} current density and also maintains its original capacitance up to 98.5% after 1.0×10^3 cycles at a 5 A g^{-1} current. Having a power density of 100 W kg^{-1}, it offers a greater energy content of up to 38.5 W h kg^{-1} while retaining 60% of its initial capacitance. By coating PPy on MnO_2 NPs that were placed on CNT cloth, Yun *et al.*[248] attempted to increase the energy output and cycle dependability. The SCs with these ternary NCs also showed remarkable flexible capacity. These ternary composite-based electrode materials demonstrated significant use in SCs.[249] Table 3 shows the development made towards improving the electrochemical performance of SCs.

CP-based electrodes used in SCs and their modification were discussed by Wustoni *et al.*[250] In another research, intrinsic CPs combined with MO NP-based electrode materials were designed and fabricated to improve the performance of SCs.[251] The probable reason for electrode material degradation with an increase in cycle life was also investigated. The reason for electrode surface rupture and degradation in the mechanical stability of electrode materials with cycle life was poor linking between metal NPs and CPs. The MO NPs start rupturing from the electrode surface with an increase in the charge/discharge cycle.

In another research, flexible SCs based on CNT-based electrodes were reported.[252] The fiber fabrics (FF) were used in CNT-

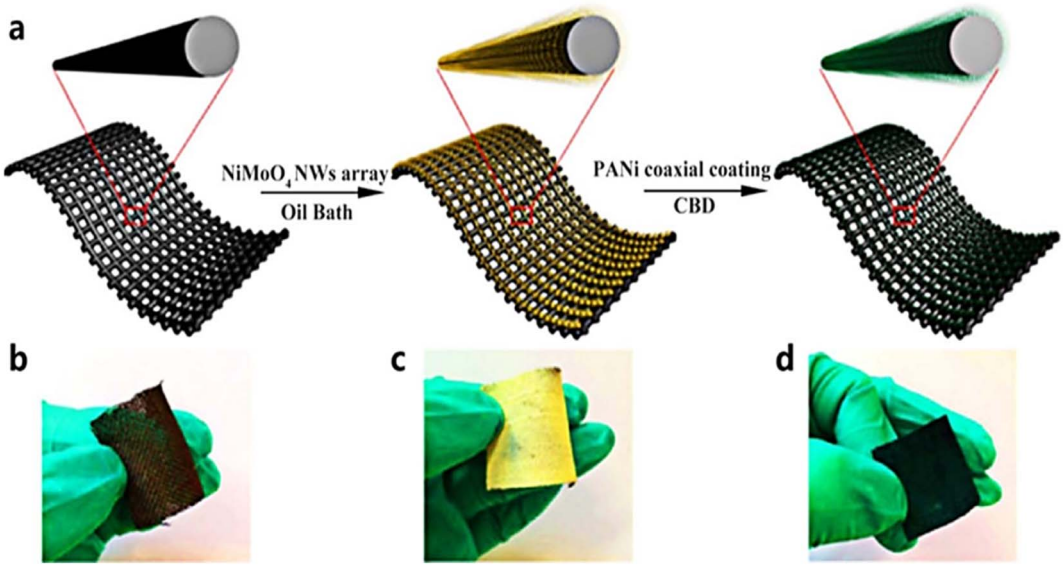

Fig. 13 (a) Representation of a fabrication process for carbon cloth/PANI/$NiMoO_4$, (b) digital photo of pristine carbon cloth, and (c) digital view of carbon cloth/PANI/$NiMoO_4$ and (d) final product of carbon cloth/PANI/$NiMoO_4$ [Reproduced with permission from ref. 242. A copyright of Elsevier, 2015].

Table 3 Progress made toward the development of different MO, CP, and CNT-based SCs

Type of electrode material used	Specific capacitance achieved (F g^{-1})	Current density	Specific surface area (m^2 g^{-1})	Reference
AC	300	0.5 A g^{-1}	3000	88
Graphene	550	0.1 A g^{-1}	2630	97
GO	349	—	—	111
RuO NFs	2000	—	—	121
CNFs/RuO/PBI	1060	0.5 A g^{-1}	678	125
MnO_2	1375	—	—	127
MnO_2/PCNFs	290	—	1815	140
MnO_2/CNTs	965	—	—	146
NiO/citric acid	338	0.5 A g^{-1}	—	148
CNFs/NiO	852	—	—	158
Co_3O_4	3560	—	485	160
$CoMnO_2$/VG CNFs	630	0.1 A g^{-1}	—	165
GO/V_2O_5	455	—	—	167
V_2O_5/CNFs	745	0.5 A g^{-1}	—	168
PANI/GN	482	0.1 A g^{-1}	—	199
PANI/MnO_2	350	1.0 A g^{-1}	872	203
PPy/$FeCl_3$	578	0.2 A g^{-1}	—	208
CNT/PPy	638	1.0 mA cm^{-2}	—	209
PPy/CoO	2225	1.0 mA cm^{-2}	612	221
PPy/MnO_2	405	1.0 A g^{-1}	—	215
PPy/CuO	1276	2.6 A cm^{-3}	478	217
PTh/TiO_2	1533	—	—	228
PTh/$LiClO_4$	255			232
Graphite/PTh/benzylidine	298			236
Carbon/PANI/$NiMnO_4$	1340	1 mA cm^{-2}		244
PANI/MWCNT/MnO_2	530	0.1 A g^{-1}		248

based electrodes to increase the flexibility of SCs. The functionalization of electrode materials was done with MnO_2 NPs. Ogihara *et al.* reported an intercalated MOF-based active electrode material for Li-ion-based ESDs.[253] They used 0.8 V potential for intercalation of Li-ions in the MOF matrix. This hybrid ESD shows an 85% retention capacity at 400 mA g^{-1}. The performance of this hybrid ESD was compared with that of an AC-based positive electrode, which shows 91% capacity retention even after 1000 discharge/charge cycles at a current of 0.15 A cm^{-2}. Brunet Cabré *et al.* have reported Ti/C/T/MXene electrode-based PSCs.[254] The Ti metal was used instead of Li metal for de-intercalation/intercalation reactions. The acidic medium was used as an electrolyte. Deprotonation/protonation of the oxygen functional group on the surface of the MXene-based electrode was followed. The capacity retention of MXene in the presence of Ti ions was found to be higher than that of CNT and CP-based ESDs.

Zhang *et al.* have reported integrated electrochemical SCs for portable ESDs used in drones and E-vehicles.[255] They have fabricated heavy load-bearing integrated ESDs comprised of electrochemical capacitors based on polymeric solid-state electrolytes. They observed an ED of 0.131 W h m^{-2}, power density of 0.13 W m^{-2}, and specific capacitance of 32.5 F cm^{-2}. Li *et al.* have reported 2D and 3D porous material MXene hydrogel-based PSCs for high-performance ESDs.[256] The different MXene used in PSCs are Mo/Ti/C/T_x, Ti/C/T_x, and Nb/C/T_x. 3D MXene-based porous materials show large SSA, good electrical conductivity, and mechanical properties. PSCs show a high specific capacitance of 230 F g^{-1} at 10 V s^{-1} or 3.32 F cm^{-2} at 10 mV s^{-1}, high ED of 9.3 × 10^{-6} W h cm^{-2}, and power density of 7.0 mW cm^{-2}.

Liang *et al.* have reported novel semiconductor-based electrode materials for advanced SCs.[257] The performance of semiconductor-based electrode materials was compared with that of AC, CNT, and CP-based electrode materials. The performance of Si and MO-based semiconductor electrode materials was found to be almost comparable to that of AC-based electrode materials but was lesser than that of CP, CNT, and MXene-based electrode materials of SCs. Panwar *et al.* have reported a MoS_2/graphene-based electrode material for ultrathin SCs.[258] They used the field effect transistor (FET) concept in their SCs. They prepared a few atomic thick layers of MoS_2/graphene in FET-based SCs. A gel electrolyte was used between the two electrodes of FETs of SCs. They observed that on combining MoS_2/graphene, the capacitance increases to 3000% in contrast to MoS_2 in the absence of graphene, which shows an 18% increase in capacitance.

Biswas *et al.* have reported anthraquinone/polydiacetylene-based asymmetric SCs.[259] They observed an increase in electrochemical performance in terms of high capacity retention (>90%), specific capacitance (340 F g^{-1}) and ED, and power density. Panwar *et al.* have fabricated FET-based SCs comprised of MoS_2/graphene.[258] They compared the electrochemical performance of ultrathin SCs with that of MoS_2 and graphene electrode material-based SCs. They observed that electrochemical performance increases almost 1000 times when combining MoS_2/graphene.

Ma *et al.* investigated the aging behavior of SCs with an increase in charging/discharging cycles.[260] This aging behavior (deterioration) of the electrode surface with an increase in the

discharge/charge cycle of SCs was based on the nature and composition of electrode materials used in SCs. The performance of single-material-based electrodes was found to be better with an increase in cycle life as compared to composite electrode material-based SCs.

In general, the ternary NCs improved specific capacitance, ED, power density, cycle stability, and other properties, especially using different CNTs. Several parameters, including electrical and thermal conductivity, internal resistance, and the kind of CNTs, CPs, and metal oxides, were utilized, which have an impact on the electrochemical and mechanical characteristics of ternary composites. Researchers were able to produce more effective ternary NC electrode materials for SCs by adjusting the different features. The effect of AC on the performance of SCs was comparable to MnO_2/PCNF-based electrodes used in SCs. A high theoretical capacity of 3000 F g^{-1} was not attained experimentally in the case of PPy/CoO-based SCs. The maximum specific capacitance observed was 2225 F g^{-1} in PPy/CoO NC-based SCs. The Co_3O_4 when used alone shows a very high specific capacitance of NiO 710 F g^{-1} with a specific area of 485 m^2 g^{-1}. Out of the three investigated CPs that is PANI, PPy, and PTh, the PPy-based composite material shows good electrochemical performance in comparison to the two other CPs. The performance of SWCNTs and MWCNTs is almost comparable with some better results in the case of SWCNTs. The influence of graphene and GO on the performance of SCs was not up to mark. But when the carbon-based cloth was used with PANI/$NiMoO_4$ its performance increased appreciably.

By combining MO, CPs, and CNTs into ternary nanocomposites, the resulting electrode materials of SCs can achieve a synergistic effect, maximizing their specific capacitance, electrical conductivity, cycling stability, and power density. The precise composition, morphology, and fabrication methods of these NCs can be tailored to optimize the desired properties for specific SC applications.

The use of nanomaterials like CNTs, graphene, MO NPs, and CPs in electrode materials for SCs increases their stability by different mechanisms.[261–263] A few important are as follows: (i) nanomaterials typically have a large surface area-to-volume ratio. This increases the number of active sites for electrochemical reactions, thus facilitating better charge storage and faster ion diffusion, (ii) nanomaterials show good electrical conductivity compared to their bulk material. This property reduces the internal resistance of the SCs, leading to increased charge and discharge rates and overall improved stability, (iii) the unique structural properties of nanomaterials contribute to increased mechanical strength. This is crucial for maintaining the structural integrity of the electrode material during repeated charge–discharge cycles, leading to a longer lifespan of SCs, (iv) nanomaterials offer better electrochemical performance, *i.e.*, higher capacitance and energy density. This results in more efficient and stable SCs, (v) nanomaterials are often more resistant to volume changes during the charge–discharge process. This minimizes electrode swelling and shrinking, reducing the likelihood of mechanical degradation and maintaining stability with time of operation, (vi) the nanoscale features of nanomaterials facilitate better accessibility for ions, improving ion diffusion and reducing the chances of concentration polarization. This leads to more consistent and stable performance of the SCs, and (vii) nanomaterials can be easily modified or functionalized to tailor their surface properties. This allows for better control over interactions with electrolytes and ions, optimizing the electrode–electrolyte interface and enhancing stability.

In a nutshell, the incorporation of nanomaterials in SC electrodes addresses different challenges, including increased surface area, improved conductivity, enhanced mechanical strength, and optimized electrochemical performance. These factors collectively contribute to the stability and longevity of SCs (Table 4).

5. Future perspective

SCs have an encouraging future in ESDs. In future SCs will improve to be very essential and beneficial in terms of the following: (i) high power density: SCs to be developed in future will deliver and store energy at a much higher rate as compared to rechargeable batteries (LIBs), making them suitable for applications in rapid energy requiring equipment/machinery, (ii) rapid charging: futuristic SCs will be charged and discharged quickly, enabling shorter charging times for ESDs and electric vehicles (EVs), (iii) long cycle life: new generation SCs will have a longer lifespan than traditional rechargeable batteries, with the ability to undergo 100 s to 1000 s of charge–discharge cycles without significant degradation, (iv) increased

Table 4 Different nanomaterials, and electrolytes used and their impact on the performance of SCs

Nanomaterial	Type of electrolyte used	Impact of electrolyte on the performance of SCs	References
Carbon and CNTs	Aqueous (*e.g.*, H_2SO_4)	(i) High surface area for increased capacitance (ii) Good electrical conductivity for fast charge/discharge (iii) Enhanced stability due to mechanical strength	90–94 and 262–267
Transition metal dichalcogenides (*e.g.*, MoS_2)	Ionic liquids	(i) High specific capacitance and energy density (ii) Improved stability in non-aqueous environments (iii) Slower ion diffusion may affect charge/discharge rates	268–270
MXene nanosheets	Aqueous (*e.g.*, Na_2SO_4)	(i) High conductivity and large surface area (ii) Good stability and mechanical strength (iii) Suitable for environmentally friendly aqueous systems (iv) Promising for high-performance supercapacitors	15, 39 and 271–274

efficiency: future research should focus on to improve the ED of SCs, allowing them to store more energy per unit volume or weight, which would enhance their overall efficiency, (v) hybrid energy storage systems: future of SCs lies in combining SCs with other energy storage technologies, such as rechargeable batteries, which can create hybrid systems that take advantage of both technologies, providing higher EDs and power output, (vi) grid energy storage: in future, SCs can play a role in developing grid-scale energy storage systems, providing fast-response power to stabilize the grid during peak demand or intermittent renewable energy generation, (vii) portable electronics: future of SCs also lies in increasing the performance of portable electronic devices by providing quick bursts of power during high-demand activities, improving user experience and reducing reliance on batteries, (viii) SC materials: future research of SCs will be focused on developing advanced materials with higher capacitance and EDs, such as graphene and CNT-based electrodes, which could lead to significant advancements in SC technology, (ix) sustainable energy storage: futuristic SCs will also provide environmental benefits as they do not rely on rare earth materials or heavy metals typically used in rechargeable batteries. Their longer lifespan and recyclability contribute to a more sustainable energy storage solution, and (x) integration with renewable energy: futuristic SCs can also help in addressing the intermittent nature of renewable sources of energy like wind, and solar by storing energy during low-demand periods and releasing it at peak demand, facilitating a more reliable and stable renewable energy grid.

In a nutshell, SCs have great potential as ESDs, offering high power density, rapid charging, long cycle life, and the ability to integrate with other technologies, making them suitable for numerous applications in the future.

6. Conclusions

SCs or ultracapacitors are ESDs that bridge the gap between traditional capacitors and rechargeable batteries, especially LIBs. They offer higher power density and faster charge–discharge rates compared to rechargeable batteries while providing higher EDs than conventional capacitors. The specific capacitance is a crucial parameter that determines the energy storage capacity of SCs. Researchers have made significant progress in improving the specific capacitance of SCs. By utilizing advanced materials, such as C-based nanomaterials (such as graphene, CPs, and CNTs) and transition MO, a high specific capacitance was achieved in the range of 10 to a few 100 F g^{-1}. The cut-off power density in the range of 100 to a few 1000 W kg^{-1} has been reported for SCs. These values demonstrate their potential use in large power appliances, like regenerative braking in electric vehicles, peak power leveling in renewable energy systems, and various other power-intensive applications.

Out of the three investigated CPs that is PANI, PPy, and PTh, the PPy-based composite material shows good electrochemical performance in comparison to PANI and PTh CPs. The performance of SWCNTs and MWCNTs is almost comparable with some better results in the case of SWCNTs. The influence of graphene and GO on the performance of SCs was not up to mark. But when the carbon-based cloth was used with PANI/$NiMoO_4$ its performance increased appreciably.

Advancements in electrode design, including nanostructuring and hierarchical architectures, have contributed to improved power density in SCs. The development of new electrolytes, SWCNTs, MWCNTs, and CPs has led to increased ionic mobility and faster charge–discharge rates of SCs. Latest developments in electrode materials for SCs include the use of (i) C-based materials, such as AC, CNTs, and graphene (G, rGO, and GO), which have a high SSA, excellent electrical conductivity, and good chemical stability, (ii) transition MO, such as RuO_2, MnO_2, and NiO, which have shown high specific capacitance, (iii) CPs, including PANI, PPy, PTh, *etc.*, which have been reported as electrode materials for SCs. These CP-based electrode materials exhibit high electrical conductivity and redox activity, (iv) MOF-based electrode materials in SCs. MOFs possess high surface areas and tuneable structures, offering potential for SC applications, and (v) 2D materials: in addition to graphene, other 2D materials, like TMDs and MXenes, have emerged as promising candidates for SC electrodes. These materials offer high surface areas, excellent electrical conductivity, and unique electrochemical properties, which can enhance the energy storage performance of SCs.

Abbreviations

CNTs	Carbon Nanotubes
SCs	Supercapacitors
EDs	Energy Densities
EDLCs	Electrical Double Layer Capacitors
ESDs	Energy Storage Devices
MO	Metal Oxide
NPs	Nanoparticles
NCs	Nanocomposites
PCs	Pseudo Capacitors
HCs	Hybrid Capacitors
ES	Electrospinning
BET	Brunauer–Emmett–Teller
R_{ct}	Charge Transfer Resistance
SSA	Specific Surface Area
ESR	Equivalent Series Resistance
PVP	Polyvinyl Pyrrolidone
PEO	Polyethylene Oxide
PVA	Polyvinyl Alcohol
PAN	Polyacrylo Nitrile
PVDF	Polyvinylidene Fluoride
AC	Activated Carbon
CMG	Chemically Modified Graphene
GO	Graphene Oxide
NFs	Nanofibers
TMDs	Transition Metal Dichalcogenides
MOFs	Metal–Organic Frameworks
DL	Double Layer
CPs	Conducting Polymers
PANI	Polyaniline
PPy	Polypyrrole
PTh	Polythiophene

SWCNTs	Single-Walled Carbon Nanotubes
MWCNTs	Multiwalled Carbon Nanotubes
LIBs	Lithium-Ion batteries
C_{dl}	Double Layer Capacitance
CVD	Chemical Vapour Deposition
CNFs	Carbon Nano Fibres
PVAC	Polyvinyl Acetate
FSCs	Flexible Supercapacitors
GNFs	Graphene Nano Fibres
CV	Cyclic Voltammetry
PMMA	Polymethyl Methacrylate
CFSs	Carbon Fibre Sheets
PCNFs	Porous Carbon Nano Fibres
EIS	Electrochemical Impedance Spectroscopy
rGO	Reduced Graphene Oxide
DCDAP	Dicyanodiamide
VGCNFs	Vapour Grown Carbon Nano Fibres
CB	Conduction Band
VB	Valence Band
ICPs	Intrinsic Conducting Polymers
GNs	Graphene Nanoplates
UPD	Underpotential Deposition

Author contributions

Aarti Tundwal: validation; and writing – original draft. Harish Kumar: conceptualization; supervision; formal analysis; data curation; validation; investigation; resources; experimental design; and writing – review and editing. Bibin J. Binoj: writing; formal analysis; and validation. Rahul Sharma: formal analysis; and validation. Gaman Kumar: formal analysis; and validation. Rajni Kumari: formal analysis; and validation. Ankit Dhayal: formal analysis; and validation. Abhiruchi Yadav: data curation; and validation. Devender Singh: data curation; and validation. Parvin Kumar: formal analysis; and validation.

Conflicts of interest

There are no conflicts to declare.

Acknowledgements

It is not possible to complete this manuscript for us without acknowledging the specific research support provided to us by CUH authorities. We duly acknowledge all types of research support provided by CUH authorities for writing this review article.

References

1 R. Tawn and J. Browell, *Renewable Sustainable Energy Rev.*, 2022, **153**, 111758.
2 D. R. Rolison, J. W. Long, J. C. Lytle, A. E. Fischer, C. P. Rhodes, T. M. McEvoy, M. E. Bourga and A. M. Lubers, *Chem. Soc. Rev.*, 2009, **38**, 226–252.
3 Z. Zhao, K. Xia, Y. Hou, Q. Zhang, Z. Ye and J. Lu, *Chem. Soc. Rev.*, 2021, **50**, 12702–12743.
4 A. S. Aricò, P. Bruce, B. Scrosati, J. M. Tarascon and W. V. Schalkwijk, *Nat. Mater.*, 2005, **4**, 366–377.
5 W. Wu, L. Yang, S. Chen, Y. Shao, L. Jing, G. Zhao and H. Wei, *RSC Adv.*, 2015, **5**, 91645–91653.
6 *Leyden Jar Electrical Instrument*, [online], available: **https://www.britannica.com/technology/Leyden-jar**.
7 R. Sharma, H. Kumar, G. Kumar, S. Sharma, R. Aneja, A. K. Sharma, R. Kumar and P. Kumar, *Chem. Eng. J.*, 2023, **468**, 143706, DOI: **10.1016/j.cej.2023.143706**.
8 E. Dhandapani, T. Sadhasivam, K. P. Ramesh, K. P. Ramesh, R. Vasudevan and N. Duraisamy, *J. Energy Storage*, 2022, **52**, 104937.
9 K. K. Patel, T. Singhal, V. Pandey, T. P. Sumangala and M. S. Sreekanth, *J. Energy Storage*, 2021, **44**, 103366.
10 M. I. A. Abdel Maksoud, R. A. Fahim, A. E. Shalan, M. A. Elkodous, S. O. Olojede, A. I. Osman, C. Farrell, A. H. Al-Muhtaseb, A. S. Awed, A. H. Ashour and D. W. Rooney, *Environ. Chem. Lett.*, 2020, **19**, 375–439.
11 M. Bigdeloo, E. Kowsari, A. Ehsani, A. Chinnappan, S. Ramakrishna and R. A. Akbari, *J. Energy Storage*, 2021, **37**, 102474.
12 P. Forouzandeh, V. Kumaravel and S. C. Pillai, *Catalysts*, 2020, **10**, 969.
13 S. Trasatti and G. Buzzanca, *J. Electroanal. Chem. Interfacial Electrochem.*, 1971, **29**, A1–A5.
14 S. Suriyakumar, P. Bhardwaj, A. N. Grace and A. M. Stephan, *Batteries Supercaps*, 2021, **4**, 571–584.
15 M. R. Lukatskaya, S. Kota, Z. Lin, M. Q. Zhao, N. Shpigel, M. D. Levi, J. Halim, P.-L. Taberna, M. W. Barsoum, P. Simon and Y. Gogotsi, *Nat. Energy*, 2017, **2**, 17105.
16 N. S. Shaikh, S. B. Ubale, V. J. Mane, J. S. Shaikh, V. C. Lokhande, S. Praserthdam, C. D. Lokhande and P. Kanjanaboos, *J. Alloys Compd.*, 2022, **893**, 161998.
17 O. Vasile, *AIP Conf. Proc.*, 2014, **1597**, 98–120.
18 A. Afif, S. M. Rahman, A. T. Azad, J. Zaini, M. A. Islan and A. K. Azad, *J. Energy Storage*, 2019, **25**, 100852.
19 Y. Kumar, A. Gupta, A. K. Thakur, S. J. Uke, V. Khatri, A. Kumar, M. Gupta and Y. Kumar, *J. Nanopart. Res.*, 2021, **23**, 119.
20 M. V. Kiamahalleh, S. H. S. Zein, G. Najafpour, S. A. Sata and S. Buniran, *Nano*, 2012, **7**, 1230002.
21 E. Herrero, L. J. Buller and H. D. Abruña, *Chem. Rev.*, 2001, **101**, 1897–1930.
22 M. Jayalakshmi and K. Balasubramanian, *Int. J. Electrochem. Sci.*, 2008, **3**, 1196–1217.
23 M. S. Halper and J. C. Ellenbogen, *Supercapacitors: A Brief overview*, The MITRE Corporation, McLean, Virginia, USA, 2006.
24 H. Choi and H. Yoon, *Nanomaterials*, 2015, **5**, 906–936.
25 P. Simon and Y. Gogotsi, *Nat. Mater.*, 2008, **7**, 845–854.
26 H. Y. Lee and J. B. Goodenough, *J. Solid State Chem.*, 1999, **144**, 220–223.
27 H. Shirakawa, E. J. Louis, A. G. MacDiarmid, C. K. Chiang and A. J. Heeger, *J. Chem. Soc. Chem. Commun.*, 1977, **578**.
28 M. Gholamian, J. Sundaram and A. Q. Contractor, *Langmuir*, 1987, **3**, 741–744.

29 S. M. Ata, Adv. Mat. Fabricat. Methods Electrochem. Supercapacitors, Dissertion, McMaster University, Canada, 2012.
30 S. Fleischmann, J. B. Mitchell, R. Wang, C. Zhan, D. Jiang, V. Presser and V. Augustyn, *Chem. Rev.*, 2020, **120**, 6738–6782.
31 A. M. Bryan, L. M. Santino, Y. Lu, S. Acharya and J. d'Arcy, *Chem. Mater.*, 2016, **28**, 5989–5998.
32 S. Mohapatra, A. Acharya and G. Roy, *Lat.-Am. J. Phys. Educ.*, 2012, **6**, 380–384.
33 S. M. Chen, R. Ramachandran, V. Mani and R. Saraswathi, *Int. J. Electrochem. Sci.*, 2014, **9**, 4072–4085.
34 A. Taleb, M. Afaq, H. A. Albalwi, F. Ismail, A. Irshad and M. M. Ibrahim, *Mater. Sci. Eng. B*, 2024, **299**, 116916, DOI: 10.1016/j.mseb.2023.116916.
35 R. Jerome and A. K. Sundramoorthy, *Anal. Chim. Acta*, 2020, **1132**, 110–120, DOI: 10.1016/j.aca.2020.07.060.
36 H. Shehzad, J. Chen, M. T. Shuang, Z. Liu, Z. H. Farooqi, A. Sharif, E. Ahmed, L. Zhou, A. Irfan, R. Begum, F. Iqbal and J. Ouyang, *Colloids Surf., A*, 2024, **680**, 132637, DOI: 10.1016/j.colsurfa.2023.132637.
37 B. Lee, S. Cho, B. J. Jeong, S. H. Lee, D. S. Kim, S. H. Kim, J.-H. Park, H. K. Yu and J. Choi, *Sens. Actuators, B*, 2024, **401**, 134913, DOI: 10.1016/j.snb.2023.134913.
38 K. Naoi and P. Simon, *Electrochem. Soc. Interface*, 2008, **17**, 34–37.
39 H. Lv, Q. Pan, Y. Song, X.-X. Liu and T. Liu, *Nano-Micro Lett.*, 2020, **12**, 118.
40 B. E. Conway, *J. Electrochem. Soc.*, 1991, **138**, 1539.
41 Z. Hadi, J. Y. Khademzadeh, Y. Zare, M. T. Munir and K. Y. Rhee, *J. Mater. Res. Technol.*, 2024, **28**, 4229–4238, DOI: 10.1016/j.jmrt.2024.01.014.
42 S. P. Nagalingam and A. N. Grace, *Mater. Today Chem.*, 2022, **26**, 101113, DOI: 10.1016/j.mtchem.2022.101113.
43 F. Guo, Y. Wang, K. Xue, L. Liu, J. Li and Y. Huang, *Compos. Sci. Technol.*, 2024, 110425, DOI: 10.1016/j.compscitech.2023.110425.
44 Y. Lv, S. Huang and Y. Zhao, *Sci. Adv. Mater.*, 2019, **11**, 418–424.
45 Z. Zhang, S. Mu, B. Zhang, L. Tao, S. Huang, Y. Huang, F. Gao and Y. Zhao, *J. Mater. Chem. A*, 2016, **4**, 2137–2146.
46 J. He, T. Tao, F. Yang and Z. Sun, *ChemSusChem*, 2022, **15**, e202200817.
47 J. Li, J. Fleetwood, W. B. Hawley and W. Kays, *Chem. Rev.*, 2021, **122**, 903–956.
48 A. Cresce and K. Xu, *Carbon Energy*, 2021, **3**, 721–751.
49 Y. Chen, T. Wang, H. Tian, D. Su, Q. Zhang and G. Wang, *Adv. Mater.*, 2021, **33**, 2003666.
50 M. N. Rantho, M. J. Madito, K. O. Oyedotun, D. J. Tarimo and N. Manyala, *AIP Adv.*, 2020, **10**, 065113, DOI: 10.1063/5.0011862.
51 G. Yu, L. Hu, N. Liu, H. Wang, M. Vosgueritchian, Y. Yang, Y. Cui and Z. Bao, *Nano Lett.*, 2011, **11**, 4438–4442.
52 Y. Zhu, S. Murali, M. D. Stoller, K. J. Ganesh, W. Cai, P. J. Ferreira, A. Pirkle, R. M. Wallace, K. A. Cychosz, M. Thommes, D. Su, E. A. Stach and R. S. Ruoff, *Science*, 2011, **332**, 1537–1541.
53 N. Lingappan, S. Lim, G. H. Lee, H. V. Tung, V. H. Luan and W. Lee, *Funct. Compos. Struct.*, 2022, **4**, 012001.
54 J. V. Patil, S. S. Mali, A. S. Kamble, C. S. Hong, J. S. Kim and P. S. Patil, *Appl. Surf. Sci.*, 2017, **423**, 641–674.
55 D. Tian, X. Lu, W. Li, Y. Li and C. Wang, *Acta Phys.-Chim. Sin.*, 2020, **36**, 1904056.
56 M. A. A. M. Abdah, N. H. N. Azman and S. Kulandaivalu, *Mater. Des.*, 2020, **186**, 108199.
57 X. Li, Y. Chen, H. Huang, Y. W. Mai and L. Zhou, *Energy Storage Mater.*, 2016, **5**, 58–92.
58 S. Peng, L. Li, J. K. Y. Lee, L. Tian, M. Srinivasan, S. Adams and S. Ramakrishna, *Nano Energy*, 2016, **22**, 361–395.
59 L. Xiang Ye, B. Tian-Jiao, W. Xin, Z. Bing, Y. Zhen-Zhen and H. Tie-Shi, *Prog. Chem.*, 2020, **33**, 1159–1174.
60 S. Bhoyate, P. K. Kahol, B. Sapkota, S. Mishra, F. Perez and R. K. Gupta, *Surf. Coat. Technol.*, 2018, **345**, 113–122.
61 A. A. M. A. Abdah, N. M. Rahman and Y. Sulaiman, *Ceram. Int.*, 2019, **45**, 8433–8439.
62 M. M. Modawe, S. Kulandaivalu, N. M. Rahman and Y. Sulaiman, *Int. J. Hydrogen Energy*, 2018, **43**, 17328–17337.
63 C. Ma, R. Wang, Z. Xie, H. Zhang, Z. Li and J. Shi, *J. Porous Mater.*, 2017, **24**, 1437–1445.
64 Q. Liu, J. Zhu, L. Zhang and Y. Qiu, *Renewable Sustainable Energy Rev.*, 2018, **81**, 1825–1858.
65 M. A. A. Mohd Abdah, N. A. Zubair, N. H. N. Azman and Y. Sulaiman, *Mater. Chem. Phys.*, 2017, **192**, 161–169.
66 S. Nur, S. Mamat, S. A. Rasyid, Z. Zainal and Y. Sulaiman, *Electrochim. Acta*, 2018, **261**, 548–556.
67 S. Nur, S. Mamat, S. A. Rasyid, Z. Zainal and Y. Sulaiman, *J. Polym. Sci., Part A: Polym. Chem.*, 2017, **56**, 50–58.
68 M. A. A. Mohd Abdah, N. A. Rahman and Y. Sulaiman, *Electrochim. Acta*, 2018, **259**, 466–473.
69 J. Yan, J. H. Choi and Y. U. Jeong, *Mater. Des.*, 2018, **139**, 72–80.
70 J. K. Gan, Y. S. Lim, A. Pandikumar, N. M. Huang and H. N. Lim, *RSC Adv.*, 2015, **5**, 12692–12699.
71 S. K. Nataraj, K. S. Yang and T. M. Aminabhavi, *Prog. Polym. Sci.*, 2012, **37**, 487–513.
72 S. Peng, L. Li, J. Kong Yoong Lee, L. Tian, M. Srinivasan, S. Adams and S. Ramakrishna, *Nano Energy*, 2016, **22**, 361–395.
73 H. Feng, H. Hu, H. Dong, Y. Xiao, Y. Cai, B. Lei, Y. Liu and M. Zheng, *J. Power Sources*, 2016, **302**, 164–173.
74 L. Qie, W. Chen, H. Xu, X. Xiong, Y. Jiang, F. Zou, X. Hu, Y. Xin, Z. Zhang and Y. Huang, *Energy Environ. Sci.*, 2013, **6**, 2497.
75 C. Huang, C. T. Hsieh, P. C. Kuo and H. Teng, *J. Mater. Chem.*, 2012, **22**, 7314.
76 D. Lee, J. Y. Jung, M. J. Jung and Y. S. Lee, *Chem. Eng. J.*, 2015, **263**, 62–70.
77 M. S. A. Rahaman, A. F. Ismail and A. Mustafa, *Polym. Degrad. Stab.*, 2007, **92**, 1421–1432.
78 D. Zhu, C. Xu, N. Nakura and M. Matsuo, *Carbon*, 2002, **40**, 363–373.
79 Z. Zhai, L. Zhang, T. Du, B. Ren, Y. Xu, S. Wang, J. Miao and Z. Liu, *Mater. Des.*, 2022, **221**, 111017.

80 H. Yang, S. Kannappan, A. S. Pandian, J. H. Jang, Y. S. Lee and W. Lu, *Nanotechnology*, 2017, **28**, 445401.
81 Z. Bo, Z. Wen, H. Kim, G. Lu, K. Yu and J. Chen, *Carbon*, 2012, **50**, 4379–4387.
82 A. Singh, N. Tiwari, P. B. Karandikar, and A. Dubey, *Internat. Conf. on Industrial Instrumentation and Control (ICIC)*, 2015, DOI: **10.1109/iic.2015.7150826**.
83 N. Syarif, *Int. Trans. J. Eng., Manage., Appl. Sci. Technol.*, 2012, **3**, 21–34.
84 A. G. Pandolfo and A. F. Hollenkamp, *J. Power Sources*, 2006, **157**, 11–27.
85 A. Khamkeaw, T. Asavamongkolkul, T. Perngyai, B. Jongsomjit and M. Phisalaphong, *Molecules*, 2020, **25**, 4063.
86 Y. Yang, K. Ge, S. Ur Rehman and H. Bi, *Rare Met.*, 2022, **41**, 3957–3975.
87 K. Lota, A. Sierczyńska, I. Acznik and G. Lota, *Chemik*, 2013, **67**, 1138–1145.
88 F. Lufrano and P. Staiti, *Int. J. Electrochem. Sci.*, 2010, **5**, 903–916.
89 Y. Cai, Z. Qin and L. Chen, *Prog. Nat. Sci.: Mater. Int.*, 2011, **21**, 460–466.
90 D. J. Tarimo, K. O. Oyedotun, N. F. Sylla, A. A. Mirghni, N. M. Ndiaye and N. Manyala, *J. Energy Storage*, 2022, **51**, 104378, DOI: **10.1016/j.est.2022.104378**.
91 P. Tamilarasan, A. Kumar Mishra, and S. Ramaprabhu, *2011 Int. Conf. on Nanoscience, Technology and Societal Implications*, 2011, pp. 1–5.
92 C. Du and N. Pan, *Nanotechnol. Law Bus.*, 2007, **4**, 3, **http://ningpan.net/publications/101-150/125.pdf**.
93 M. G. Sumdani, M. R. Islam, A. N. A. Yahaya and S. I. Safie, *Polym. Eng. Sci.*, 2021, **62**, 269–303.
94 M. S. Halper and J. C. Ellenbogen, *Supercapacitors: A brief overview*, The MITRE Corporation, McLean, Virginia, USA, 2006.
95 J. Li, X. Cheng, A. Shashurin and M. Keidar, *Graphene*, 2012, **1**, 1–13.
96 C. Marcano, D. V. Kosynkin, J. M. Berlin, A. Sinitskii, Z. Sun, A. Slesarev, L. B. Alemany, W. Lu and J. M. Tour, *ACS Nano*, 2010, **4**, 4806–4814.
97 I. Ahmad, R. Pawara, R. Girase, A. Pathan, V. Jagatap, N. C. Desai, Y. O. Ayipo, S. J. Surana and H. Patel, *ACS Omega*, 2022, **7**, 21820–21844.
98 C. H. Wu, J. Zhu, B. Zhang, H. Shi, H. Zhang, S. Yuán, Y. Yu, G. Chen and C. Chen, *J. Colloid Interface Sci.*, 2023, **650**, 1871–1880.
99 M. Fu, W. Chen, Y. Lei, H. Yu, Y. Lin and M. Terrones, *Adv. Mater.*, 2023, **35**, 2300940.
100 J. Rajendran, A. K. Sundramoorthy, D. Ganapathy, R. Atchudan, M. A. Habila and D. Nallaswamy, *J. Hazard. Mater.*, 2022, **440**, 129705.
101 P. Karthika, N. Rajalakshmi and K. S. Dhathathreyan, *Soft Nanosci. Lett.*, 2012, **2**, 59–66.
102 T. Kim, G. J. Jung, S. M. Yoo, K. S. Suh and R. S. Ruoff, *ACS Nano*, 2013, **7**, 6899–6905.
103 T. Y. Kim, H. W. Lee, M. Stoller, D. R. Dreyer, C. W. Bielawski, R. S. Ruoff and K. S. Suh, *ACS Nano*, 2010, **5**, 436–442.
104 K. C. Moon, Z. B. Li, Y. D. Yao, Z. Lin, Q. Liang, J. C. Agar, M. Song, M. Liu, and C. P. Wong, *Proceedings 60th Electronic Components and Technology Conference (ECTC)*, 2010, DOI: **10.1109/ectc.2010.5490644**.
105 D. J. Tarimo, K. O. Oyedotun, A. A. Mirghni and N. I. Manyala, *Int. J. Hydrogen Energy*, 2020, **45**, 13189–13201, DOI: **10.1016/j.ijhydene.2020.03.059**.
106 R. Ramachandran, M. Saranya, V. Velmurugan, B. P. C. Raghupathy, S. K. Jeong and A. N. Grace, *Appl. Energy*, 2015, **153**, 22–31.
107 F. Zhang, K. Yang, G. Liu, Y. Chen, M. Wang, S. Li and R. Li, *Composites, Part A*, 2022, **160**, 107051.
108 T. Kuilla, S. Bhadra, D. Yao, N. H. Kim, S. Bose and J. H. Lee, *Prog. Polym. Sci.*, 2010, **35**, 1350–1375.
109 M. A. Pope, S. Korkut, C. Punckt and I. A. Aksay, *J. Electrochem. Soc.*, 2013, **160**, A1653–A1660.
110 Z. S. Iro, *Int. J. Electrochem. Sci.*, 2016, **11**, 10628–10643.
111 W. Lv, D. M. Tang, Y. B. He, C. H. You, Z. Q. Shi, X. C. Chen, C. M. Chen, P.-X. Hou, C. Liu and Q. H. Yang, *ACS Nano*, 2009, **3**, 3730–3736.
112 J. Yan, J. Liu, Z. Fan, T. Wei and L. Zhang, *Carbon*, 2012, **50**, 2179–2188.
113 R. Lakra, R. Kumar, P. K. Sahoo, D. Thatoi and A. Soam, *Inorg. Chem. Commun.*, 2021, **133**, 108929.
114 R. Liang, Y. Du, P. Xiao, J. Cheng, S. Yuan, Y. Chen, J. Yuan and J. Chen, *Nanoscale Adv.*, 2021, **3**, 6294–6309.
115 T. E. Balaji, H. Tanaya Das and T. Maiyalagan, *ChemElectroChem*, 2021, **8**, 1723–1746.
116 J. Zheng, R. Zhang, P. S. Yu and X. F. Wang, *J. Alloys Compd.*, 2019, **772**, 359–365.
117 Z. Zhang, Z. Xu, Z. Yao, Y.-Q. Meng, Q. Xia and D. Li, *J. Alloys Compd.*, 2019, **805**, 396–403.
118 S. Mothkuri, S. Chakrabarti, H. Gupta, B. Padya, T. N. Rao and P. K. Jain, *Mater. Today: Proc.*, 2020, **26**, 142–147.
119 T. F. Yi, J. Mei, B. Guan, P. Cui, S. Luo, Y. Xie and Y. Liu, *Ceram. Int.*, 2020, **46**, 421–429.
120 J. Lin, Y. Yan, H. Wang, X. Zheng, Z. Jiang, Y. Wang, S. Ding, J. Cao, W. Fei and J. Feng, *J. Alloys Compd.*, 2019, **794**, 255–260.
121 C. C. Hu, K. H. Chang, M. C. Lin and Y. T. Wu, *Nano Lett.*, 2006, **6**, 2690, DOI: **10.1021/nl061576a**.
122 L. Q. Chen, Y. Hou, J. H. Kang, A. Hirata, T. Fujita and M. Chen, *Adv. Energy Mater.*, 2013, **3**, 851–856, DOI: **10.1002/aenm.201300024**.
123 Y. Xu, J. Wei, L. Tan, J. Yu and Y. Chen, *J. Mater. Chem. A*, 2015, **3**, 7121–7131.
124 J. J. Jhao, C. H. Lin, T. K. Yeh, H. C. Wu, M. C. Tsai and C. K. Hsieh, *Surf. Coat. Technol.*, 2017, **320**, 263–269.
125 B. H. Kim, C. D. Kim and G. S. Lee, *J. Electroanal. Chem.*, 2016, **760**, 64–70.
126 B. K. Balan, H. D. Chaudhari, U. K. Kharul and S. Kurungot, *RSC Adv.*, 2013, **3**, 2428, DOI: **10.1039/C2RA22776B**.

127 K. S. Yang, Y. W. Joo, K. T. Chan, J. H. Kim, and W. J. Lee, in *Proc. 10th WSEAS Int. Conf. on Computers*, 2006, pp. 888–892.
128 M. Toupin, T. Brousse and D. Bélanger, *Chem. Mater.*, 2004, **16**, 3184–3190, DOI: 10.1021/cm049649j.
129 Y. Liu, M. Liu, P. Zheng, D. Ge and L. Yang, *Mater. Des.*, 2019, **182**, 108022, DOI: 10.1016/j.matdes.2019.108022.
130 A. V. Radhamani, M. Krishna Surendra and M. S. Ramachandra Rao, *Mater. Des.*, 2018, **139**, 162–171.
131 W. Wei, X. Cui, W. Chen and D. G. Ivey, *Chem. Soc. Rev.*, 2011, **40**, 1697–1721.
132 J. Shin, J. K. Seo, R. Yaylian, A. Huang and Y. S. Meng, *Int. Mater. Rev.*, 2019, **65**, 356–387.
133 N. Yu, H. Yin, W. Zhang, Y. Liu, Z. Tang and M.-Q. Zhu, *Adv. Energy Mater.*, 2015, **6**, 1501458.
134 X. Song, H. Wang, Z. Li, C. Du and R. Guo, *Chem. Rec.*, 2022, **22**, e202200118.
135 T. Yue, B. Shen and P. Gao, *Renewable Sustainable Energy Rev.*, 2022, **158**, 112131.
136 S. A. Klankowski, G. P. Pandey, G. Malek, C. R. Thomas, S. L. Bernasek, J. Wu and J. Li, *Nanoscale*, 2015, **7**, 8485–8494.
137 Y. Wen, T. Qin, Z. Wang, X. Jiang, S. Peng, J. Zhang, J. Hou, F. Huang, D. He and G. Cao, *J. Alloys Compd.*, 2017, **699**, 126–135.
138 O. Pech and S. Maensiri, *J. Alloys Compd.*, 2019, **781**, 541–552, DOI: 10.1016/j.jallcom.2018.12.088.
139 D. Zhou, H. Lin, F. Zhang, H. Niu, L. Cui, Q. Wang and F. Qu, *Electrochim. Acta*, 2015, **161**, 427–435.
140 N. H. Kwon, K.-G. Lee, H. K. Kim and S. J. Hwang, *Mater. Chem. Front.*, 2021, **5**, 3549–3575.
141 H. Xu, S. Li, J. Yang and J. Hu, *J. Colloid Interface Sci.*, 2018, **513**, 448–454.
142 C. M. Yang and B. H. Kim, *J. Alloys Compd.*, 2019, **780**, 428–434.
143 H. Z. Chi, H. Zhu and L. Gao, *J. Alloys Compd.*, 2015, **645**, 199–205.
144 D. G. Lee and B.-H. Kim, *Synth. Met.*, 2016, **219**, 115–123.
145 A. Śliwak and G. Gryglewicz, *Energy Technol.*, 2014, **2**, 819–824.
146 L. Wang, M. M. Huang, S. Chen, L. P. Kang, X. He, Z. Lei, F. Shi, H. Xu and Z.-H. Liu, *J. Mater. Chem. A*, 2017, **5**, 19107–19115.
147 Y. Yang, F. Yang, H. Hu, S. Lee, Y. Wang, H. Zhao, D. Zeng, B. Zhou and S. Hao, *Chem. Eng. J.*, 2017, **307**, 583–592.
148 S. Zhang, Y. Pang, Y. Wang, B. Dong, S. Lu, M. Li and S. Ding, *J. Alloys Compd.*, 2018, **735**, 1722–1729.
149 B.-S. Yin, Q. Wang, S.-W. Zhang, C. Liu, Q. Ren and K. Ke, *ACS Appl. Mater. Interfaces*, 2016, **8**, 26019–26029.
150 G. Cheng, W. Yang, C. Dong, T. Kou, Q. Bai, H. Wang and Z. Zhang, *J. Mater. Chem. A*, 2015, **3**, 17469–17478.
151 Y. Wang, S. Huang, Y. Lu, S. Cui, W. Chen and L. Mi, *RSC Adv.*, 2017, **7**, 3752–3759.
152 K. S. Hui, K. S. Hui, K. S. Hui and K. S. Kim, *J. Mater. Chem. A*, 2016, **4**, 9113–9123.
153 G. Zhu, J. Chen, Z. Zhang, Q. Kang, X. Feng, Y. Li, Z.-D. Huang, L. Wang and Y. Ma, *Chem. Commun.*, 2016, **52**, 2721–2724.
154 R. Wang, D. Jin, Y. Zhang, S. Wang, J. Lang, X. Yan and L. Zhang, *J. Mater. Chem. A*, 2017, **5**, 292–302.
155 L. Zang, J. Zhu and Y. Xia, *J. Mater. Eng. Perform.*, 2013, **23**, 679–683.
156 M. Kundu and L. Liu, *Mater. Lett.*, 2015, **144**, 114–118.
157 Q. Li, J. Guo, D. Xu, J. Guo, X. Ou, Y. Hu, H. Qi and F. Yan, *Small*, 2018, **14**, 1704203, DOI: 10.1002/smll.201800426.
158 S. Aloqayli, C. K. Ranaweera, Z. Wang, K. Siam, P. K. Kahol, P. Tripathi, O. N. Srivastava, B. K. Gupta, S. R. Mishra, F. Perez, X. Shen and R. K. Gupta, *Energy Storage Mater.*, 2017, **8**, 68–76.
159 S. J. Mammadyarova, *Azerb. Chem. J.*, 2021, **2**, 80–93.
160 S. Ameen, M. S. Akhtar, H.-K. Seo, Y. S. Kim and H. S. Shin, *Chem. Eng. J.*, 2012, **187**, 351–356.
161 X. Wang, A. Hu, C. Meng, C. Y. Wu, S. Yang and X. Hong, *Molecules*, 2020, **25**, 269.
162 D. Majumdar and S. Ghosh, *J. Energy Storage*, 2020, **34**, 101995.
163 M. Yaseen, M. A. K. Khattak, M. Humayun, M. Usman, S. S. Shah, S. Bibi, B. S. U. Hasnain, S. M. Ahmad, A. Khan, N. Shah, A. A. Tahir and H. Ullah, *Energies*, 2021, **14**, 7779.
164 J. E. Kim, Y. G. Ko, S. Y. Lee, D. Y. Lee, S. W. Kim, Y. Kim and C.-C. Yang, *Int. J. Electrochem. Sci.*, 2022, **46**, 23564–23577.
165 J. Bhagwan, V. Sivasankaran, K. L. Yadav and Y. Sharma, *J. Power Sources*, 2016, **327**, 29–37, DOI: 10.1016/j.jpowsour.2016.07.040.
166 Y. Ju, X. Liu, X. Ye, M. Dai, B. Fang, X. Shen and L. Liu, *ACS Appl. Nano Mater.*, 2023, **6**, 13792–13823.
167 N. M. Ndiaye, B. D. Ngom, N. F. Sylla, T. M. Masikhwa, M. J. Madito, D. Momodu, T. Ntsoane and N. Manyala, *J. Colloid Interface Sci.*, 2018, **532**, 395–406.
168 R. Thangappan, S. Kalaiselvam, A. Elayaperumal and R. Jayavel, *Solid State Ionics*, 2014, **268**, 321–325.
169 B. H. Kim, C. H. Kim, K. S. Yang, A. Rahy and D. J. Yang, *Electrochim. Acta*, 2012, **83**, 335–340.
170 G. Huang, C. Li, J. Bai, X. Sun and H. Liang, *Int. J. Hydrogen Energy*, 2016, **41**, 22144–22154.
171 T. Prasankumar, V. S. Irthaza Aazem, P. Raghavan, K. Prem Ananth, S. Biradar, R. Ilangovan and S. P. Jose, *J. Alloys Compd.*, 2017, **695**, 2835–2843.
172 S. J. Uke, S. P. Mardikar, A. Kumar, Y. Kumar, M. Gupta and Y. Kumar, *R. Soc. Open Sci.*, 2021, **8**, 210567, DOI: 10.1098/rsos.210567.
173 M. G. Tadesse, E. Kasaw, B. Fentahun, E. Loghin and J. F. Lübben, *Energies*, 2022, **15**, 2471.
174 H. Mu, J. Bai, C. Li and W. Sun, *J. Alloys Compd.*, 2019, **775**, 872–882.
175 R. Holze, *Polymers*, 2020, **12**, 1835.
176 V. V. Kondratiev and R. Holze, *Chem. Pap.*, 2021, **75**, 4981–5007.
177 S. Banerjee, K. Kar and K. Das, *Recent Pat. Mater. Sci.*, 2014, **7**, 173–203.

178 M. Samtham, D. Singh, K. Hareesh and R. S. Devan, *J. Energy Storage*, 2022, **51**, 104418.
179 R. Holze, *Molecules*, 2022, **27**, 546.
180 S. Banerjee and K. Kar, *Recent Pat. Mater. Sci.*, 2014, **7**, 131–150.
181 Z. Li and L. Gong, *Materials*, 2020, **13**, 548.
182 D. Li, J. Huang and R. B. Kaner, *Acc. Chem. Res.*, 2008, **42**, 135–145.
183 S. R. Sivakumar, W. J. Kim, J. A. Choi, D. R. MacFarlane, M. Forsyth and D. W. Kim, *J. Power Sources*, 2007, **171**, 1062–1068.
184 H. Li, J. Wang, Q. Chu, Z. Wang, F. Zhang and S. Wang, *J. Power Sources*, 2009, **190**, 578–586, DOI: **10.1016/j.jpowsour.2009.01.052**.
185 J. Xu, K. Wang, S. Z. Zu, B. H. Han and Z. Wei, *ACS Nano*, 2010, **4**, 5019–5026.
186 C. Bavatharani, E. Muthusankar, S. M. Wabaidur, Z. A. Alothman, K. M. Alsheetan, M. Mana AL-Anazy and D. Ragupathy, *Synth. Met.*, 2021, **271**, 116609.
187 S. P. Nagalingam and A. N. Grace, *Mater. Today Chem.*, 2022, **26**, 101113.
188 H. Wang, Y. Diao, Y. Lu, H. Yang, Q. Zhou, K. Chrulski and J. M. D'Arcy, *Nat. Commun.*, 2020, **11**, 3882.
189 Z. Zhao, G. F. Richardson, Q. Meng, S. Zhu, H.-C. Kuan and J. Ma, *Nanotechnology*, 2015, **27**, 042001.
190 M. N. Gueye, A. Carella, J. Faure-Vincent, R. Demadrille and J.-P. Simonato, *Prog. Mater. Sci.*, 2020, **108**, 100616.
191 C. Meng, C. Liu, L. Chen, C. Hu and S. Fan, *Nano Lett.*, 2010, **10**, 4025–4031.
192 A. Imani and G. Farzi, *J. Mater. Sci.: Mater. Electron.*, 2015, **26**, 7438–7444.
193 Z. Niu, P. Luan, Q. Shao, H. Dong, J. Li, J. Chen, D. Zhao, L. Cai, W. Zhou, X. Chen and S. Xie, *Energy Environ. Sci.*, 2012, **5**, 8726.
194 H. Mi, X. Zhang, S. An, X. Ye and S. Yang, *Electrochem. Commun.*, 2007, **9**, 2859–2862.
195 C. Tran, R. Singhal, D. Lawrence and V. Kalra, *J. Power Sources*, 2015, **293**, 373–379.
196 K. Zhang, L. L. Zhang, X. S. Zhao and J. Wu, *Chem. Mater.*, 2010, **22**, 1392–1401.
197 A. Kausar, *Mater. Res. Innovations*, 2021, **26**, 1–13.
198 O. Okhay and A. Tkach, *Nanomaterials*, 2022, **12**, 2531.
199 A. M. Díez-Pascual, *Polymers*, 2021, **13**, 2978.
200 X. Cai, K. Sun, Y. Qiu and X. Jiao, *Crystals*, 2021, **11**, 947.
201 R. Vinodh, R. S. Babu, S. Sambasivam, C. V. V. M. Gopi, S. Alzahmi, H.-J. Kim, A. L. F. de Barros and I. M. Obaidat, *Nanomaterials*, 2022, **12**, 1511.
202 H. Gómez, M. K. Ram, F. Alvi, P. Villalba, E. Stefanakos and A. Kumar, *J. Power Sources*, 2011, **196**, 4102–4108.
203 A. H. Gemeay, I. A. Mansour, R. G. El-Sharkawy and A. B. Zaki, *Eur. Polym. J.*, 2005, **41**, 2575–2583.
204 X. Zhang, L. Ji, S. Zhang and W. Yang, *J. Power Sources*, 2007, **173**, 1017–1023.
205 L. Chen, L.-J. Sun, F. Luan, Y. Liang, Y. Li and X.-X. Liu, *J. Power Sources*, 2010, **195**, 3742–3747.
206 Q. Yang, Z. Hou and T. Huang, *J. Appl. Polym. Sci.*, 2014, **132**, 41615, DOI: **10.1002/app.41615**.
207 M. Li and L. Yang, *J. Mater. Sci.: Mater. Electron.*, 2015, **26**, 4875–4879.
208 J. Xu, D. Wang, L. Fan, Y. Yuan, W. Wei, R. Liu, S. Gu and W. Xu, *Org. Electron.*, 2015, **26**, 292–299.
209 M. Rajesh, C. Justin Raj, B.-G. Kim, B.-B. Cho and J. M. Ko, *Electrochim. Acta*, 2016, **220**, 373–383.
210 Q. Tang, M. Chen, C. Yang, W. Wang, H. Bao and G. Wang, *Chem. Mater.*, 2015, **7**, 15303–15313.
211 L. Yang, Z. Shi and W. Yang, *Electrochim. Acta*, 2015, **153**, 76–82.
212 Y. Chen, L. Du, P. Yang, P. Sun, X. Yu and W. Mai, *J. Power Sources*, 2015, **287**, 68–74.
213 H. Wang, Y. Zhang, H. Ang, Y. Zhang, H. Tan, Y. Zhang, Y. Guo, J. C. Franklin, X.-L. Wu, S. Madhavi, H. J. Fan and Q. Yan, *Adv. Funct. Mater.*, 2016, **26**, 3082–3093.
214 L. Cao, F. Xu, Y. Y. Liang and H.-L. Li, *Adv. Mater.*, 2004, **16**, 1853–1857.
215 J. S. Shayeh, S. O. R. Siadat, M. Sadeghnia, K. Niknam, M. Rezaei and N. Aghamohammadi, *J. Mol. Liq.*, 2016, **220**, 489–494.
216 J. Ji, X. Zhang, J. Liu, L. Peng, C. Chen, Z. Huang, L. Li, X. Yu and S. Shang, *Mater. Sci. Eng., B*, 2015, **198**, 51–56.
217 W. Ji, Y. Zhang, X. Cui, J. Chen, D. Liu, H. Deng and Q. Fu, *Chem. Commun.*, 2015, **51**, 7669–7672.
218 T. Qian, J. Zhou, N. Xu, T. Yang, X. Shen, X. Liu, S. Wu and C. Yan, *Nanotechnology*, 2015, **26**, 425402.
219 F. Wang, X. Zhan, Z. Cheng, Z. Wang, Q. Wang, K. Xu, M. Safdar and J. He, *Small*, 2014, **11**, 749–755.
220 M. Yu, Y. Zeng, Y. Han, X. Cheng, W. Zhao, C. Liang, Y. Tong, H. Tang and X. Lu, *Adv. Funct. Mater.*, 2015, **25**, 3534–3540.
221 X. Sun, Q. Li and Y. Mao, *Electrochim. Acta*, 2015, **174**, 563–573.
222 R. J. Choudhary, S. Ansari and B. Purty, *J. Energy Storage*, 2020, **29**, 101302.
223 C. Zhou, Y. Zhang, Y. Li and J. Liu, *Nano Lett.*, 2013, **13**, 2078–2085, DOI: **10.1021/nl400378j**.
224 S. Patil, N. R. Chodankar, Y. S. Huh and D. W. Lee, *J. Power Sources*, 2020, **453**, 227766.
225 G. A. Snook, P. Kao and A. S. Best, *J. Power Sources*, 2011, **196**, 1–12.
226 L. Nyholm, G. Nyström, A. Mihranyan and M. Strømme, *Adv. Mater.*, 2011, **23**, 3751–3769.
227 B. Senthilkumar, P. Thenamirtham and R. Kalai Selvan, *Appl. Surf. Sci.*, 2011, **257**, 9063–9067.
228 A. Laforgue, P. Simon, C. Sarrazin and J.-F. Fauvarque, *J. Power Sources*, 1999, **80**, 142–148.
229 R. B. Ambade, S. B. Ambade, R. R. Salunkhe, V. Malgras, S. H. Jin, Y. Yamauchi and S.-H. Lee, *J. Mater. Chem. A*, 2016, **4**, 7406–7415.
230 R. Prabhu, M. Rajasekhar and A. Subramanian, *Int. J. Electrochem. Sci.*, 2009, **4**, 1289–1301.
231 S. R. P. Gnanakan, N. Murugananthem and K. Dai, *Polym. Adv. Technol.*, 2009, **22**, 788–793.
232 S. Nejati, T. E. Minford, Y. Y. Smolin and K. K. S. Lau, *ACS Nano*, 2014, **8**, 5413–5422.

233 B. H. Patil, A. D. Jagadale and C. D. Lokhande, *Synth. Met.*, 2012, **162**, 1400–1405.
234 A. Alabadi, S. Razzaque, Z. Dong, W. Wang and B. Tan, *J. Power Sources*, 2016, **306**, 241–247.
235 C. Fu, H. Zhou, R. Liu, Z. Huang, J. Chen and Y. Kuang, *Mater. Chem. Phys.*, 2012, **132**, 596–600.
236 H. Q. Zhang, Z. Hu, M. Li, L.-W. Hu and S. Jiao, *Mater. Chem. Phys.*, 2014, **2**, 17024–17030.
237 J. Xiao, H. Li, H. Zhang, S. He, Q. Zhang, K. Liu, S. Jiang, A. Greiner and K. Zhang, *J. Bioresour. Bioprod.*, 2022, **7**, 245–269.
238 Q. Lu and Y. Zhou, *J. Power Sources*, 2011, **196**, 4088–4094.
239 R. B. Ambade, S. B. Ambade, N. K. Shrestha, Y. C. Nah, S.-H. Han, W. Lee and S. H. Lee, *Chem. Commun.*, 2013, **49**, 2308.
240 A. R. Akbar, W. Tian, M. I. Qadir, Z. Khaliq, Z. Liu, M. Tahir, Y. Hu, C. Xiong and Q. Yang, *Colloids Surf., A*, 2021, **610**, 125644.
241 Y. Li, C. Zhu, T. Lu, Z. Guo, D. Zhang, J. Ma and S. Zhu, *Carbon*, 2013, **52**, 565–573.
242 Y. Chen, B. Liu, Q. Liu, J. Wang, J. Liu, H. Zhang, S. Hu and X. Jing, *Electrochim. Acta*, 2015, **178**, 429–438.
243 M. M. Sk, C. Y. Yue and R. K. Jena, *Synth. Met.*, 2015, **208**, 2–12.
244 X. Wang, P. Xu, P. Zhang and S. Ma, *Materials*, 2021, **14**, 7148.
245 C. H. Ng, H. N. Lim, Y. S. Lim, W. K. Chee and N. M. Huang, *Int. J. Energy Res.*, 2014, **39**, 344–355.
246 L. Jiang, X. Lu, C. Xie, G. Wan, H. Zhang and T. Youhong, *J. Phys. Chem. C*, 2015, **119**, 3903–3910.
247 W. K. Chee, H. San Lim, I. Harrison, M. Ali, Z. Zainal, C. R. Ng and N. Huang, *Electrochim. Acta*, 2015, **157**, 88–94.
248 T. G. Yun, B. Il Hwang, D. Kim, S. Hyun and S. M. Han, *ACS Appl. Mater. Interfaces*, 2015, **7**, 9228–9234.
249 D. Majumdar, *ChemElectroChem*, 2020, **8**, 291–336.
250 S. Wustoni, D. Ohayon, A. Hermawan, A. Nuruddin, S. Inal, Y. S. Indartono and B. Yuliarto, *Polym. Rev.*, 2023, 1–59.
251 M. Ikram and R. Holze, *Polymers*, 2023, **15**, 730.
252 Y. Han, H. Ha, C. Choi, H. Yoon, P. Matteini, J. Cheong and S. Hwang, *Appl. Sci.*, 2023, **13**, 5290.
253 N. Ogihara, M. Hasegawa, H. Kumagai, R. Mikita and N. Nagasako, *Nat. Commun.*, 2023, **14**, 1472.
254 M. Brunet Cabré, D. Spurling, P. Martinuz, M. Longhi, C. Schröder, H. Nolan, V. Nicolosi, P. E. Colavita and K. McKelvey, *Nat. Commun.*, 2023, **14**, 374.
255 J. Zhang, J. Yan, Y. Zhao, Q. Zhou, Y. Ma, Y. Zi, A. Zhou, S. Lin, L. Liao, X. Hu and H. Bai, *Nat. Commun.*, 2023, **14**, 64.
256 K. Li, J. Zhao, A. Zhussupbekova, C. E. Shuck, L. Hughes, Y. Dong, S. Barwich, S. Vaesen, I. V. Shvets, M. Möbius, W. Schmitt, Y. Gogotsi and V. Nicolosi, *Nat. Commun.*, 2022, **13**, 6884.
257 C. Liang, S. Wang, S. Sha, S. Lv, G. Wang, B. Wang, Q. Li, J. Yu, X. Xu and L. Zhang, *J. Mater. Chem. C*, 2023, **11**, 4288–4317.
258 V. Panwar, P. S. Chauhan, S. Kumar, R. Tripathi and A. Misra, *ACS Energy Lett.*, 2023, **8**, 1510–1519.
259 S. Biswas, N. Shauloff, R. Bisht and R. Jelinek, *Adv. Sustainable Syst.*, 2023, **7**, 2370018.
260 N. Ma, D. Yang, S. Riaz, L. Wang and K. Wang, *Technologies*, 2023, **11**, 38.
261 W. K. Chee, H. N. Lim, Z. Zainal, N. M. Huang, I. Harrison and Y. Andou, *J. Phys. Chem. C*, 2016, **120**, 4153–4172.
262 J. Rajendran, A. N. Reshetilov and A. K. Sundramoorthy, *RSC Adv.*, 2021, **11**, 3445–3451.
263 Y. Han, Y. Ge, Y. Chao, C. Wang and G. G. Wallace, *J. Energy Chem.*, 2018, **27**, 57–72.
264 Z. S. Iro, C. Subramani, J. Rajendran and A. K. Sundramoorthy, *Carbon Lett.*, 2021, **31**, 237.
265 M. Halim, G. Liu, R. E. A. Ardhi, C. Hudaya, O. Wijaya, S. H. Lee, A. Y. Kim and J. K. Lee, *ACS Appl. Mater. Interfaces*, 2017, **9**, 20566–20576.
266 M. X. Tran, A. Kim and J. K Lee, *Appl. Surf. Sci.*, 2018, **461**, 161–170.
267 A.-Y. Kim, R. E. A. Ardhi, G. Liu, J. Y. Kim, H. J. Shin, D. Byun and J. K. Lee, *Carbon*, 2019, **153**, 62–72.
268 L. Li, Z. Wei, J. Liang, J. Ma and S. Huang, *Results Chem.*, 2021, **3**, 100205.
269 M. Acerce, D. Voiry and M. Chhowalla, *Nat. Nanotechnol.*, 2015, **10**, 313–318.
270 L. Khandare, D. J. Late and N. B. Chaure, *Front. Chem.*, 2023, **11**, DOI: **10.3389/fchem.2023.1166544**.
271 S. A. Thomas, A. Patra, B. M. Al-Shehri, M. Selvaraj, A. Aravind and C. S. Rout, *J. Energy Storage*, 2022, **55**, 105765.
272 S. Kumar, M. A. Rehman, S. Lee, M. Kim, H. Hong, J. Y. Park and Y. Seo, *Sci. Rep.*, 2021, **11**, 649.
273 R. Ma, Z. Chen, D. Zhao, X. Zhang, J. Zhuo, Y. Yin, X. Wang, G. Yang and F. Yi, *J. Mater. Chem. A*, 2021, **9**, 11501–11529.
274 Y. Ying, Q. Fan, Z. Li and P. Fu, *Mater. Today Sustain.*, 2023, **24**, 100551.